*International Journal of Advanced Technology and Engineering Exploration, Vol 10(107)*
*ISSN (Print): 2394-5443 ISSN (Online): 2394-7454*
*http://dx.doi.org/10.19101/IJATEE.2023.10101035*

**Research Article**

# Feasibility and stability of preview control for 2-D discrete-time systems described by the Roesser model

**Akhilesh Kumar Ravat[1*], Amit Dhawan[2], Manish Tiwari[3] and Sumit Kumar Jha[4]**
Research Scholar, Department of Electronics and Communication Engineering, MNNIT Allahabad, Prayagraj, 211004, Uttar Pradesh, India[1]
Professor, Department of Electronics and Communication Engineering, MNNIT Allahabad, Prayagraj, 211004, Uttar Pradesh, India[2]
Associate Professor, Department of Electronics and Communication Engineering, MNNIT Allahabad, Prayagraj, 211004, Uttar Pradesh, India[3]
Assistant Professor, Department of Electronics and Communication Engineering, MNNIT Allahabad, Prayagraj, 211004, Uttar Pradesh, India[4]

Received: 12-January-2023; Revised: 16-October-2023; Accepted: 19-October-2023


## Abstract
***Feasibility and stability were deemed crucial for preview controller design in a two-dimensional (2-D) discrete-time (DT) system. In this paper, the feasibility and stability of preview control for the 2-D DT system described by the Roesser model with disturbances were studied. The underlying system involved the difference between a system state and its steady-state value, as opposed to the usual difference between system states typically utilized in past literature. An (AE) system was constructed in this paper, in which the augmented state variables not only contained error signals and preview information but also included a discrete integrator for the elimination of static errors. The AE system included a reference signal's future information and a disturbance signal to achieve the regulator problem from the existing tracking problem. Based on Lyapunov stability theory, a new linear matrix inequality (LMI)-based criterion was derived, ensuring the feasibility and stability of the derived AE system. Furthermore, a state feedback control law with a design approach of the preview control process was proposed based on the LMI method. The proposed controller was utilized to perform preview tracking control for the 2-D system while achieving the asymptotic stability of the overall closed-loop system. Finally, numerical examples were provided to demonstrate the advantages of the proposed method. MATLAB software and the yet another linear matrix inequality parser (YALMIP) toolbox were used to determine the controller gain matrix.***

## Keywords
***Preview control, YALMIP, Linear matrix inequality (LMI), Discrete-time system, State feedback, Roesser model, Lyapunov function, Augmented error (AE) system.***

## 1.Introduction
In preview control systems, it is crucial to make sure that outputs accurately follow the reference signal whenever there are external disturbances. Preview control approaches have included a variety of techniques that have been used to solve the difficulties of maintaining accurate tracking and successfully rejecting interruptions. With the availability of advanced knowledge of the future state of the reference signal, one can significantly enhance the transient response of the system.

The term "preview control" typically refers to a class of anticipatory control processes with a preview period which extends into the future [1–2].

The authors in [3, 4] have discussed the tracking of wheeled robots, humanoids, robotic cars, and bipedal walking robots using the preview control.

For real-time applications, a preview control mechanism has been shown in [5]. Sheridan has discussed three models of preview control in [6]. An optimal finite-preview controller has been formulated by Tomizuka in [7]. By using a different technique, the above-mentioned control problems have been

*Author for correspondence

solved in [8–13]. For constructing control systems, including preview control for discrete-time (DT) systems, linear matrix inequality (LMI) has been a vital tool [14].

A control design problem is reduced to a set of algebraic inequalities utilizing numerical optimization techniques based on LMI-based design methodology. LMI-based design techniques are used to identify the controller gains for preview control systems that will give the system the appropriate performance and stability characteristics. The linear quadratic gaussian (LQG) control method is a popular method for developing preview control systems employing LMI. In this approach, the control issue is formulated as a linear time-invariant (LTI) system with additive Gaussian noise, and the optimal control strategy is then solved using LMI. The reference signal’s preview data is utilized to address the tracking control issue and improve the system's tracking level and response time. Since the concept of future control has been put forward, it has been targeted at various one-dimensional (1-D) control systems. People utilized the future data to develop a controller with an information compensation function to enhance the tracking of the system. Based on LMI technology, an optimal control theory has been connected by introducing a difference operator or differential operator construction to increase the wide error system. Systems with continuous-time (CT) and those with discrete time with performance tracking based on state feedback controllers have been proposed in [15–19].

Further, the preview controller's design for tracking the control problem of a CT stochastic control system in two-dimensional (2-D) has become popular because the theoretical research results of the 2-D system have been applied to computed tomography image analysis, multidimensional digital image analysis, X-ray spectrum analysis, etc. Thus, it is crucial to take into account the 2-D system's future control issues. The Roesser model has been used to analyze and develop control systems for a variety of purposes. This has helped to mitigate the consequences of disruptions and improve the system's tracking performance. It is significant to highlight that the accuracy of the model, measurement noise, and other factors have an impact on the quality of the prediction employed in preview control, which is essential for its effectiveness. Many researchers have used the Roesser model for 2-D system controller design in [20, 21]. Many models have been used to resolve the stability problem in different areas of control systems. It has been proposed one after another, among which the Fornasini-Marchesini (FM) first model and second model have been chosen due to their structure and application advantages [22]. This article explores utilizing reference signal information to its greatest potential. To realize the tracking target of the 2-D DT system and improve the tracking performance, the state of the 2-D system changes in two directions. The construction methods of the system are according to the difference between the steady-state value and the state value. The transformation method constructs a 2-D AE system. Due to the new state containing preview information, it has an error system for augmentation. The necessary conditions for asymptotic stability are fed into and obtained through the LMI toolbox. The gain matrix of the preview controller is obtained by the desired controller. A toolset called yet another linear matrix inequality parser (YALMIP) is used to model and resolve optimization issues, notably nonlinear and linear issues with LMI constraints. It is created using MATLAB and may be used to develop and analyze controllers for a variety of systems, including hybrid and nonlinear systems. In addition to offering a user-friendly interface for defining and modifying optimization problems, YALMIP permits the use of a range of solvers, including both paid and free choices. It is an effective tool for control system design and analysis, and both academia and industry have made extensive use of it. YALMIP is first considered for semi-definite programming (SDP) and LMI. The user-defined problem is solved automatically using YALMIP and a suitable solver [23]. A representation for the Roesser model in the form of a matrix block diagram [24] is shown in *Figure 1*.

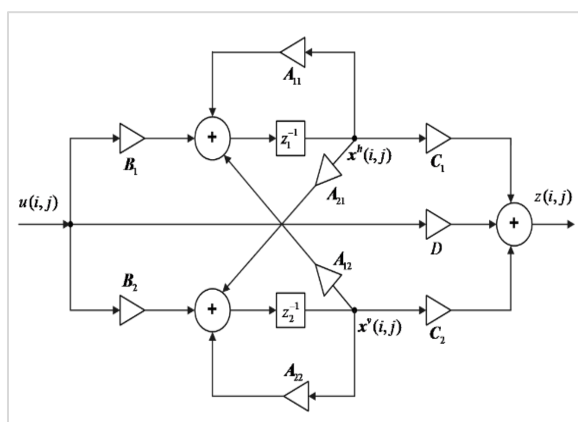


**Figure 1** A matrix block diagram representation for the Roesser model

### 1.1Challenges

Although several crucial research works have been reported in the past literature, many open challenges exist for the design of a preview controller for a DT system. These challenges can be categorized as follows:

a) Modeling: To create a successful control plan, the system's dynamics must be effectively described. If the system is complicated or not well understood, this may be challenging.
b) Complexity of calculation: The control algorithm may call for a substantial amount of computation, which makes real-time implementation on a constrained computing platform difficult.
c) Sensor limitations: The control system could be dependent on sensor readings, which might be noisy or inaccurate.
d) Preview window: The size of the preview window, or the quantity of future data used to influence control decisions, can significantly affect how well the control system performs. Finding the ideal preview window size can be challenging.
e) Robustness: The control system must be resistant to system dynamics disturbances and uncertainty.
f) Stability: The closed-loop system needs to be stable, which means that even in the face of shocks and uncertainties, the output must converge to a steady state.

### 1.2Motivation

A control method for DT systems called preview control makes use of upcoming knowledge about the system's inputs to enhance control effectiveness. The primary goal of preview control is to overcome the limitations of traditional feedback control, which can only make control decisions based on information from the present or past regarding the system's inputs. Preview control can predict disturbances and make necessary corrections before they happen, leading to improve control performance [3]. Additionally, because preview control enables the controller to consider input constraints when generating control decisions, it can be used with systems that have restrictions on the control inputs, such as systems with actuator saturation or rate limits. In preview control systems, firstly, it is important to check whether our designed controller is feasible or not. If it is feasible, typically the next step is to validate the stability of the controller. It is the most important point for 1-D systems as well as 2-D systems. Different types of research papers in the field of preview control have been reported in the literature, in which feasibility and stability were important issues [22].

However, in a 2-D preview control system, there are many research gaps to describe the feasibility and stability of preview control. The reported literature for 2-D system has only described preview controller design without disturbance. However, in DT systems, including robotics and automated manufacturing, preview control is a control method that enhances control performance by using knowledge of future system states. Utilizing knowledge of future system states to predict and compensate for disruptions, such as external forces or sensor noise, before they occur is the goal of preview control. This may result in the system being controlled more precisely, effectively, and robustly against disturbances. The system's trajectory can also be improved using preview control, for example, by reducing energy use or increasing throughput. In general, using preview control can enhance the effectiveness and performance of DT systems in a variety of applications [25, 26].

Furthermore, it is important that the outputs track the reference signal when external disturbances are present. Hence, motivated by the above research gap, this paper proposes a preview control for a 2-D DT system based on the Roesser model with disturbance.

### 1.3Objectives

The goal of this study is to quickly validate the complete use of preview data for the reference signal and disturbance signal, as well as determine the feasibility and stability of the preview control for 2-D DT systems.

In order to extend the preview control theory from a 1-D system to a 2-D system, an AE system is created where augmented state variables not only contain error signals and preview information but also include a discrete integrator introduced to eliminate static errors.

The objective of the controller is to be used for 2-D system preview tracking control to achieve asymptotic stability. The Lyapunov method derives the LMI condition for which the AE system is asymptotically stable under state feedback and gives the design of a preview controller.

### 1.4Contributions

In order to extend the preview control theory from the 1-D system to the 2-D system, an AE system is created where augmented variables not only contain error signals and preview information but also include a discrete integrator introduced to eliminate static errors. In this paper, a novel criterion is provided to guarantee the feasibility and stability of preview control for a 2-D DT system with disturbances based on the Roesser model.

Using MATALB software and the YALMIP toolbox, one can readily verify the validity of the conditions stated in Theorem 1.

The paper is structured in the manner described below. Section 1 provides the introduction, challenges, motivation, objectives and contributions of the paper. A brief review of the existing literature is discussed in Section 2. A method to construct an AE system and the design of a preview control for a 2-D system represented by the Roesser model are provided in Section 3. Section 4 and Section 5 provide detailed simulation results along with their respective discussions. Lastly, Section 6 discusses the paper's conclusion.

## 2.Literature review

This section's literature review on preview control examines the many issues and techniques for dealing with them in relation to preview control. The work in the field of preview control is divided into several categories, which are generally based on formulations of preview control problems, a domain of preview control problems, methodologies utilized for preview control problems, and lastly, objectives based on preview control problems [1–3].

The following are some readings on preview control:

➢ Preview control issues based on formulation:

Based on the formulation, the preview control problem can be categorized as follows:

(i)Formulation of the preview control in CT

(ii)Formulation of the preview control in DT

(iii)Preview control formulations based on uncertainty.

In the CT domain, Shaked and De [27] have introduced preview controllers for CT systems. For linear time-varying systems, the problem of finite-horizon H-infinity tracking is investigated using a CT-based model. Additionally, tracking control designs for time-invariant systems with zero initial conditions are produced after an analysis of tracking difficulties for time-invariant systems on infinite horizons. The issue of linear time-varying systems tracking finite horizon H-infinity is addressed using a differential game technique. Lu et al. [28] have discussed multi-agent linear CT systems for optimal preview design. First, the problem is reformulated as a collection of optimized output regulation problems using the state augmentation methodology and the topology reconstruction method. Secondly, the compensations for preview feed-forward associated with many leaders are obtained using the linear superposition approach. Thirdly, it has been shown that the various optimal regulation issues can be resolved by representing each preceding compensation term in relation to the current state of the leader. Xie et al. [29] have discussed a robust decentralized preview tracking controller for parametrically uncertain CT systems. Furthermore, the LMI is used to obtain the decentralized preview controller. The proposed control technique can increase the closed-loop system's tracking accuracy, reduce settling time, and enable the system to respond in advance, according to simulation results. The preview action extends for a set period of time; hence, the length is frequently expressed in units of time, most often seconds. The benefit of this formulation is that it allows the controller output to be provided directly to the real system.

It's crucial to keep in mind that the preview controllers were created in a DT domain, where preview action is represented by time steps when working in the DT domain. Ravat et al. [30] have outlined the implementation of a preview control system using preview horizon control. They provide a numerical simulation illustration related to the preview with the assistance of MATLAB. Negm et al. [31] have discussed a three-phase induction motor (IM) controlled by an artificial neural network (ANN) based on preview control. A three-phase IM on-line speed control approach using a global ANN is proposed. The best preview controller serves as the foundation for this algorithm. The suggested algorithm's goals are to manage the rotor speed, the field orientation, and the constant flux. Utilizing a neural network-based approach, the on-line speed management goal of IM is employed to emulate the attributes of the optimal preview controller within a comprehensive and precise performance framework. Results from digital computer simulations have been used to show the viability, dependability, and efficiency of the suggested global ANN algorithm.

The formulations for preview control in DT are more straightforward compared to their CT counterparts, as the delay element in DT is of finite dimension.

As no system can be fully explored, the most crucial component of a control system is its uncertainty-based formulation. This formulation allows for the controller model to be developed for robust performance in the presence of plant uncertainty. The authors in [32–34] have shown that for known plant uncertainties, a plant's accuracy can be further improved. The norm of uncertainty is supposed to be bound and the reference signal is predicted with a defined length. In order to create enhanced error systems, a model transformation is included to roughly represent the time-varying delay. The small gain theorem is used to determine the requirements for sliding motion that are asymptotically stable. The switching surface can be drawn to and maintained by the controlled system state according to the sliding mode preview controller's design. To demonstrate the potency of the suggested control design, a numerical example is provided. The research in [12] has provided a description of the output feed-backing of the preview control for an electromechanical valve actuator. In this research, an electromechanical engine, solenoid actuators operate the airflow control valves, removing the need for a camshaft and enabling adjustable valve timing. A linearized system model exhibits good agreement with the full model when compared to experimental data and the full simulation model. Experimental findings demonstrate the actuator control's successful performance using a preview control strategy. Furthermore, a preview tracking control for a stochastic system with retarded state multiplication is suggested by the authors in [13]. In this research, for retarded LTI systems, the issue of tracking with a preview in the presence of uncertainties of Wiener-type stochastic parameter is resolved. Recently, the input-output method has been utilized to transform delayed state systems with stochastic elements into uncertain delay-free systems bounded by norms. The comparable norm-bounded system has been applied to yield minimal control and maximizing disturbance techniques that are based on measurements of the system states and the anticipated reference data. There are two examples that highlight the effects of the delay duration and the preview length on the system achievement serve as illustrations for the theoretical findings. In [15], Takaba discussed the problem of polytopic uncertainty in the context of reliable servomechanisms with preview action. The paper addresses the design of a robust servomechanism for a system subject to polytopic uncertainty and exposed to a previewable signal. They offer a design strategy for a state feedback controller with integral and preview actions based on the robust mixed linear quadratic (LQ) criterion, attaining the robust tracking achievement in terms of LMI.

- Preview control issues based on methodology domain:

The system's features, such as the control signal, settling time, peak overshoot, error signal, etc., are defined in time analysis for time-domain methods. Design issue and model based on time are used to preview controller design in the time domain. In the time domain method, the controller design can immediately take into account the signal preview information. In [8], the authors have explored a method utilizing discrete lifting technology for delay plants using a single input. This approach is employed in the design of preview controllers for DT linear systems with multiple input delays. The design methodology is distinguished by the DT nature of the delay-accumulation feedback operator and the infinite dimensionality of the actuator dynamics. To be more precise, a new discrete lifting technique was developed to minimize the delays and turn the tracking issue becomes a regulator issue using an AE system. Analytical solutions for the relevant operator Riccati equations are used to resolve the H-infinity control issue of general preview or delayed systems. The solution of the problem can handle preview and delayed control issues. The solution helps with seeing things ahead of time and controlling delays. It can be used in a lot of systems that have delays in how they take in and send out information. The transcendental equations' roots describe the solvability requirement, and the control design for the overall issue is provided using an integro-differential observer. Based on the solvability requirement and the consequent control rule, some interpretations of typical control problems are offered in [9]. Taking into account the forward and feedback channels' delay compensations of the networked control systems, the problem of networked output tracking control is investigated. The feedback channel delay is adjusted utilizing an extended functional observer, the calculation of output delay is handled as a distinct form of output disturbance. The forward channel delay is compensated using two distinct algorithms: buffer-based and packet-based. The networked closed-loop systems are then given a stability study in [35]. Ha et al. [36] have analyzed the challenge of creating partial state observers that experience delays in both the control input and the measured output for a linear system. To guarantee exponential convergence of the observer error, a novel approach for designing a minimal-order observer is introduced. To demonstrate the design process, viability, and efficacy of the suggested strategy, numerical examples are given. Given that the delay element in DT systems has finite dimensions, the formulations of the preview control problem in DT are simpler compared to their CT counterparts.

The features of systems are described on a frequency scale in frequency-domain approaches. This approach is more crucial for systems where evaluating the frequency response is more crucial than the transient response. There are not many studies that explore designing preview controllers in the frequency domain. Kristalny and Mirkin [37] have examined the issue of stability within a comprehensive two-sided rational model matching framework, which has been explored in this study. The generic two-sided stability and its one-sided equivalent have different conceptual underpinnings. Some of these discrepancies have been proven to be irrelevant to the majority of interesting situations and may be ignored. Numerous optimization issues with asymptotic behavior limitations can be resolved by reducing the number of parameters for all the stabilizing solutions. This domain methodology proves more advantageous for systems in which analyzing the frequency response holds greater importance than assessing the transient response.

- Preview control issues based on the solution approach:

The existing control theories serve as the foundation for the traditional procedures. The preview control system's design is implemented using conventional control theories. In the classical approach, the parameter choice governs the results defined, which are known as Q, R, $\gamma$, and $\eta$. Q and R are chosen as design necessities. The values of $\gamma$ and $\eta$ are more affect the solution more. The LMIs' implementation is straightforward and produces overall results that contrast with the Riccati equation. The preview controller is proposed using a contemporary method with the aid of contemporary control algorithms like ANN and fuzzy logic. The preview data is gathered and sent to the rear suspension system by a sensor attached to the front suspension. The collected preview data and the vehicle state feedback signal are then processed using a fuzzy controller. The application of fuzzy control is intended to increase suspension robustness against sensor noise; the discussed algorithm is better than the traditional proportional integral derivative (PID) approach, according to experimental results. As a result, the suggested control algorithm can significantly increase ride comfort [38]. Wang and Aida [39] have provided a novel technique for fuzzy nonlinear preview control. There are numerous methods for preview control because it can reduce both overshoot and control energy. Fuzzy theory is used to create a new design scheme for the preview control element, which is then optimized via a genetic algorithm (GA) based on performance criteria. Because it was created using a nonlinear model, the fuzzy preview control will work better with nonlinear plants. The effectiveness of the suggested strategy is finally demonstrated by various experiments using a two-cascaded tank design.

- Preview control issues based on objective:

The reference signal with known future values should be tracked by the reference tracking issue. Robot motion, missile control, and other areas are applications for reference tracking difficulties. Before transient responses can be enhanced in terms of accuracy for tracking and input control needs, the future value of reference signals must be determined. The basic goal of disturbance reduction issues is to keep the system's output at the necessary level while a disruption exists [40–42]. Xu and Peng [40] have analyzed, a preview steering control algorithm, along with a comprehensive examination of its closed-loop system and experimental validation, ensuring precise, smooth, and cost-effective path tracking for automated vehicles. Then, a DT preview controller is created on top of a linear AE system, where the state vector is enhanced to include disturbances that occur inside a finite preview window. The path-tracking controller for automated cars may be designed or improved with the assistance of developers thanks to the design methodology, system analysis, and experimental verification given in this work. Future studies will investigate system latency and robustness to sensor and road disturbances in more detail. Xie et al. [43] have analyzed an effective preview control for perturbed CT networked systems, which is a challenging issue. They use decentralized control technologies. Each perturbed subsystem's tracking controller is initially designed. The envisioned tracking challenge is transformed into a regulatory problem by using a perturbed error system. To deal with the uncertainty in the systems, an innovative approach is suggested. The cost function in this strategy incorporates the uncertainty bound. As a result, the nominal system's preview controller can be regarded as a reliable preview controller for the perturbed subsystem. To demonstrate the usefulness and superiority of the suggested controller, a numerical example is provided.

The research work done in [44, 45] examines the gain-scheduled robust attitude control technique based on a preview obtained by using control techniques with linearly variable parameters for DT systems with one-sided Lipschitz nonlinearity. Initially, an enhanced system is constructed using a difference operator to incorporate tracking errors and preview information. Subsequently, a sliding surface is formulated, and a condition ensuring asymptotic stability is derived. To simplify the controller solution process, avoiding the need for computations involving nonlinear matrix inequalities and classification, a convex optimization problem is formulated. The linear parameter-varying controller adopts a modified PID control structure to improve the robustness performance, aligning with the robust control framework presented in [44, 45].

Stability is the main objective in the design of any control system. The most crucial step in the design of any control system is to assess the system's stability. If the system is prone to instability, a suitable controller must be created in order to stabilize the current system. It is well recognized that there may be some mistakes as a result of control system modeling assumptions whenever mathematical models are employed to explain real-world systems. Uncertain parameters are included in the intended model to reflect the impact of error. Our system has a tendency to become the system unstable because of uncertainty. In order to develop a robust controller, we must design a new kind of controller. This reliable controller can stabilize the system for all permitted parameter uncertainties. Strong system uncertainty, stability and robust performance are the two main problems of a robust controller.

Following a review of the literature on preview tracking control for a system, there are a number of key considerations:

a. A key task in the design of a control system is to check the stability of the system, and if the system is unstable, then there is a need to construct a desired control law for system stability.
b. Because of the assumptions made during the modeling process, mistakes are always present when mathematical models are employed to explain real-world systems. An unknown parameter is included to account for the impact of such inaccuracies. Because of this uncertainty, the system is unstable; hence, a trustworthy controller must be developed to maintain system stability within the allowed parameter uncertainties.
c. There are two key considerations for a robust controller:
1. Strong stability
2. Powerful performance

The controller must ensure the desired performance while maintaining stability.

d. The term "guaranteed cost control approach" refers to a strategy that ensures the desired performance. For guaranteed cost control approaches, the closed loop cost function’s upper bound is more important, and a controller in this form is referred to as an “optimal guaranteed cost controller”.
e. When implementing state feedback control, the controller gain frequently displays some jitter. The term "controller fragility" refers to a feedback control system's performance deteriorating as a result of incorrect controller implementation. The goal of non-fragile control is to create a controller for a certain system that is unaffected by a small amount of gain error.
f. In real-world control systems, delay shows up organically in states and inputs. Instabilities are primarily brought on by these delays. State delays are related to travel time, whereas input delays are the result of the transmission of measurement information and should be considered in a practical system design.

# 3.Methods

In control systems, it is crucial to evaluate the feasibility and stability of any 2-D DT system based on the Roesser model. A technique is developed to form an AE system, incorporating future knowledge regarding the reference signal and disturbance signal. This transformation obtains the regulator problem from the tracking. The output preview control gains are solved by the proposed condition.

## 3.1System descriptions

The Roesser model, a DT state-space representation of a system, is frequently used in control theory. This paper presents the design of a preview control for a 2-D DT system with disturbance based on the Roesser model [24]. Consider a system defined in Equations 1a and 1b:

$$\begin{bmatrix} \boldsymbol{x}^h(s+1,t) \\ \boldsymbol{x}^v(s,t+1) \end{bmatrix} = \begin{bmatrix} \boldsymbol{A}_{11} & \boldsymbol{A}_{12} \\ \boldsymbol{A}_{21} & \boldsymbol{A}_{22} \end{bmatrix} \begin{bmatrix} \boldsymbol{x}^h(s,t) \\ \boldsymbol{x}^v(s,t) \end{bmatrix} + \begin{bmatrix} \boldsymbol{B}_1 \\ \boldsymbol{B}_2 \end{bmatrix} u(s,t) + \begin{bmatrix} \boldsymbol{E}_1 \\ \boldsymbol{E}_2 \end{bmatrix} \boldsymbol{w}(s,t) \tag{1a}$$

$$z(s,t) = [\boldsymbol{C}_1 \quad \boldsymbol{C}_2] \begin{bmatrix} \boldsymbol{x}^{h}(s,t) \\ \boldsymbol{x}^{v}(s,t) \end{bmatrix} \tag{1b}$$

where, $\boldsymbol{x}^h(s,t) \in \boldsymbol{R}^{n_1}$ shows the horizontal state. The vertical state are represented by $\boldsymbol{x}^v(s,t) = \boldsymbol{R}^{n_2}$. Control input vector is shown by $\boldsymbol{u}(s,t) \in \boldsymbol{R}^m$. $z(s,t) \in \boldsymbol{R}^p$ is the controlled output vector and $\boldsymbol{w}(s,t) \in \boldsymbol{R}^l$ is the disturbance vector. Equation 1c shows that the constant matrix.

$$\boldsymbol{A} = \begin{bmatrix} \boldsymbol{A}_{11} & \boldsymbol{A}_{12} \\ \boldsymbol{A}_{21} & \boldsymbol{A}_{22} \end{bmatrix}, \quad \boldsymbol{B} = \begin{bmatrix} \boldsymbol{B}_1 \\ \boldsymbol{B}_2 \end{bmatrix}, \quad \boldsymbol{C} = [\boldsymbol{C}_1 \quad \boldsymbol{C}_2], \quad \boldsymbol{E} = \begin{bmatrix} \boldsymbol{E}_1 \\ \boldsymbol{E}_2 \end{bmatrix} \tag{1c}$$

Are referred to as real constant matrices having the proper size.

The boundary conditions are shown by Equation 2:

$$\boldsymbol{x}^h(0,t) = \boldsymbol{x}^h_t, \quad \boldsymbol{x}^v(s,0) = \boldsymbol{x}^v_s \text{ and } s,t = 0,1,2,3... \tag{2}$$

and $X_r = \sup\{\|x(s,t)\|\} \quad : s+t=k, \quad s,t \in \boldsymbol{Z}$,

And, $\boldsymbol{x}(s,t) = (\boldsymbol{x}^{hT}(s,t) \ \ \boldsymbol{x}^{vT}(s,t))^T$ then Equation 1a asymptotic stable 2-D DT system. This is how it is explained:

**Definition 1:** For the 2-D DT system (1) if $\lim_{k\to\infty} X_r = 0$ is true, then asymptotically stable is a term used to describe the 2-D DT system 1a. In the 1-D DT system, preview tracking control problems need to be given general assumptions about previewable information. Similarly, for the 2-D DT systems preview tracking control problem, the corresponding assumption also needs to be made.

## 3.2Assumptions

The following assumptions were used for the design of 2-D DT systems preview tracking control.

**Assumption 1:** The reference signal $\boldsymbol{r}(s,t) \in \boldsymbol{R}^P$ has the preview length of $M_r$, for discrete independent variables $(s,t)$ in the vertical and horizontal directions and the Equation 3 show the future value of DT variable:

$$s+t=k, s+t=k+1, \quad s+t=k+2, \quad s+t=k+3, \quad ... \quad s+t=k+M_r \tag{3}$$

The future value, that is greater than the preview length, is assumed to be constant vector ($\mathbf{r}^*$) this can be expressed as $s+t \geq k+M_r+1$, i.e., $\boldsymbol{r}(s,t) = \boldsymbol{r}^*$ and $\lim_{s+t\to\infty} r(s,t) = r^*$, where $\boldsymbol{r}^*$ is known as constant vector.

**Assumption 2:** Suppose the reference signal can be split as $\boldsymbol{r}(s,t) = r_1(s,t) + r_2(s,t)$, by Assumption 1, $r_1(s,t)$ and $r_2(s,t)$ can be obtained within the preview length as shown in Equation 4:

$$\lim_{s+t\to\infty} \boldsymbol{r}_1(s,t) = \boldsymbol{r}_1{}^* \tag{4}$$
$$\lim_{s+t\to\infty} \boldsymbol{r}_2(s,t) = \boldsymbol{r}_2{}^*$$

Error signal $\boldsymbol{e}(s,t) \in \boldsymbol{R}^P$ can be represented as Equation 5:

$$\boldsymbol{e}(s,t) = z(s,t) - \boldsymbol{r}(s,t) \tag{5}$$

This paper has explored the preview tracking of 2-D DT system by Equation 1a–1b. It is expected that the designed controller, the system's output z(s, t) can follow the reference signal r(s, t).

Also, $\lim_{s+t\to\infty} \boldsymbol{e}(s,t) = \lim_{s+t\to\infty}(z(s,t) - \boldsymbol{r}(s,t)) = 0$ is true.

Horizontal and vertical output of systems is shown by Equation 6:

$$z_1(s,t) = \boldsymbol{C}_1 \boldsymbol{x}^h(s,t)$$
$$z_2(s,t) = \boldsymbol{C}_2 \boldsymbol{x}^v(s,t) \tag{6}$$

Suppose $z_1(s,t)$ can track $\boldsymbol{r}_1(s,t)$, while $z_2(s,t)$ can track $\boldsymbol{r}_2(s,t)$. The steady state values of the system are given below as Equation 7:

$$\begin{cases} \lim_{s+t\to\infty} x^v(s,t) = \boldsymbol{x}_v^* \\ \lim_{s+t\to\infty} x^h(s,t) = \boldsymbol{x}_h^* \\ \lim_{s+t\to\infty} u(s,t) = u^* \end{cases} \tag{7}$$

Further, take the limit of system as Equation 1a-1b and $s+t\to\infty$ then we have obtained Equation 8.

$$\begin{cases} \boldsymbol{x}_h^* = \boldsymbol{A}_{11}\boldsymbol{x}_h^* + \boldsymbol{A}_{12}\boldsymbol{x}_v^* + \boldsymbol{B}_1 u^* \\ \boldsymbol{x}_v^* = \boldsymbol{A}_{21}\boldsymbol{x}_h^* + \boldsymbol{A}_{22}x_v^* + \boldsymbol{B}_2 u^* \\ \boldsymbol{C}_1\boldsymbol{x}_h^* = \boldsymbol{r}_1^* \\ \boldsymbol{C}_2\boldsymbol{x}_v^* = \boldsymbol{r}_2^* \end{cases} \tag{8}$$

The Equation 8 is converted into Equation 9.

$$\begin{bmatrix} \boldsymbol{A}_{11}-I & \boldsymbol{A}_{12} & \boldsymbol{B}_1 \\ \boldsymbol{A}_{21} & \boldsymbol{A}_{22}-I & \boldsymbol{B}_2 \\ \boldsymbol{C}_1 & \boldsymbol{0} & \boldsymbol{0} \\ \boldsymbol{0} & \boldsymbol{C}_2 & \boldsymbol{0} \end{bmatrix} \begin{bmatrix} \boldsymbol{x}_h^* \\ \boldsymbol{x}_v^* \\ u^* \end{bmatrix} = \begin{bmatrix} \boldsymbol{0} \\ \boldsymbol{0} \\ \boldsymbol{r}_1^* \\ \boldsymbol{r}_2^* \end{bmatrix} \tag{9}$$

Equation 9 can have at least one solution provided the following Assumption 3 is satisfied to ensure that $((\boldsymbol{x}_h^*)^T, (\boldsymbol{x}_v^*)^T, (u^*)^T)^T$ exist.

**Assumption 3:** This point guarantees the following rank condition holds.

$$rank\begin{bmatrix} A_{11}-I & A_{12} & B_1 \\ A_{21} & A_{22}-I & B_2 \\ C_1 & \mathbf{0} & \mathbf{0} \\ \mathbf{0} & C_2 & \mathbf{0} \end{bmatrix} = rank\begin{bmatrix} A_{11}-I & A_{12} & B_1 & \mathbf{0} \\ A_{21} & A_{22}-I & B_2 & \mathbf{0} \\ C_1 & \mathbf{0} & \mathbf{0} & r_1^* \\ \mathbf{0} & C_2 & \mathbf{0} & r_2^* \end{bmatrix}$$

A control variable's number should be equal to or greater than the number of independent variables. It is intended to measure. i.e., $m \geq p$.

**Assumption 4:** Suppose that preview length of disturbances $(w(s,t))$ is $M_d$; and for every time, the $M_d$ is the future length of disturbance signal. Both past and current values of exogenous disturbances are accessible. For exceeding the future value for $s+t \geq k+M_d+1$, the values of disturbance signal will be zero; i.e., $w(s,t)=0$.

In order to formulate the proposed controller for the 2-D system, the Roesser model was further analyzed and following fundamental points were derived:

a. The system was linear, indicating that its response was independent of past interactions between its input and output and that its output was proportional to its input.
b. The system was time-invariant, meaning that its properties remained constant over time and its response to any input was constant irrespective of its time of application.
c. The system was deterministic, meaning that its input and initial state totally dictated its output.
d. Because the system was represented using a DT framework, the input and output were tracked and updated at specific intervals of time.

$$\begin{cases} \tilde{\boldsymbol{x}}^h(s+1,t) = \boldsymbol{A}_{11}\tilde{\boldsymbol{x}}^h(s,t) + \boldsymbol{A}_{12}\tilde{\boldsymbol{x}}^h(s,t) + \boldsymbol{B}_1\tilde{\boldsymbol{u}}(s,t) \\ \tilde{\boldsymbol{x}}^v(s,t+1) = \boldsymbol{A}_{21}\tilde{\boldsymbol{x}}^h(s,t) + \boldsymbol{A}_{22}\tilde{\boldsymbol{x}}^v(s,t) + \boldsymbol{B}_2\tilde{\boldsymbol{u}}(s,t) \\ \boldsymbol{e}_1(s+1,t) = \boldsymbol{C}_1[\boldsymbol{A}_{11}\tilde{\boldsymbol{x}}^h(s,t) + \boldsymbol{A}_{12}\tilde{\boldsymbol{x}}^v(s,t) + \boldsymbol{B}_1\tilde{\boldsymbol{u}}(s,t)] - \widetilde{\boldsymbol{r}_1}(s+1,t) \\ \boldsymbol{e}_2(s+1,t) = \boldsymbol{C}_2[A_{21}\tilde{\boldsymbol{x}}^h(s,t) + \boldsymbol{A}_{22}\tilde{\boldsymbol{x}}^v(s,t) + \boldsymbol{B}_2\tilde{\boldsymbol{u}}(s,t)] - \widetilde{\boldsymbol{r}_2}(s,t+1) \end{cases} \quad (11)$$

From Assumption 2, we obtained the vertical and horizontal discrete variables $(s,t)$, notation of future value of time is given by Equation 12 a:

$$s+t=k, \quad s+t=k+1, \quad s+t=k+2, \ldots\ldots\ldots s+t=k+M_r \quad (12a)$$

The following Equation 12b shows the condition of reference signal.

$$s+t \geq k+M_r+1, \quad \widetilde{\boldsymbol{r}_1}(s,t) = \widetilde{\boldsymbol{r}_2}(s,t) = 0 \quad (12b)$$

The preview vector forms of $\widetilde{\boldsymbol{r}_1}(s,t)$ and $\widetilde{\boldsymbol{r}_2}(s,t)$ are given below:

$$\boldsymbol{X}_{R0}^h(s,t) = \begin{bmatrix} \widetilde{\boldsymbol{r}_1}(s,t) \\ \widetilde{\boldsymbol{r}_1}(s+1,t) \\ \vdots \\ \widetilde{\boldsymbol{r}_1}(s+M_r,t) \end{bmatrix}$$

$$\boldsymbol{X}_{R1}^{\square}(s,t) = \begin{bmatrix} \widetilde{\boldsymbol{r}_1}(s,t+1) \\ \widetilde{\boldsymbol{r}_1}(s+1,t+1) \\ \vdots \\ \widetilde{\boldsymbol{r}_1}(s+M_r-1,t+1) \end{bmatrix}$$

### 3.3AE system derivation

AE system derivation was the technique used in preview control to increase the effectiveness of the control system. A form of control system called preview control had utilized set points or future reference signals to better track the controlled variable. With the enhanced error system, a new state variable was added to the system to indicate the difference in reference signals between the present and the future. Improved tracking was achieved by adding an extra state variable to the control system, which allowed the controller to predict future reference signals and modify the control signal accordingly. We began with the system model in the form of a difference equation in order to derive the enhanced error system for preview control of a DT system. The present state value and steady-state value difference had been obtained in order to create an augmented error (AE) system. Converting the tracking issue into a regulatory issue, we derived an error system of augmentation and designed a controller for preview. Define the following new vectors as Equation 10:

$$\begin{cases} \tilde{\boldsymbol{x}}^h(s,t) = \boldsymbol{x}^h(s,t) - \boldsymbol{x}_h^* \\ \tilde{\boldsymbol{x}}^v(s,t) = \boldsymbol{x}^v(s,t) - \boldsymbol{x}_v^* \\ \tilde{\boldsymbol{u}}(s,t) = \boldsymbol{u}(s,t) - \boldsymbol{u}^* \\ \widetilde{\boldsymbol{r}_1}(s,t) = \boldsymbol{r}_1(s,t) - \boldsymbol{r}_1{}^* \\ \widetilde{\boldsymbol{r}_2}(s,t) = \boldsymbol{r}_2(s,t) - \boldsymbol{r}_2{}^* \end{cases} \quad (10)$$

The system's state equation can be expressed as follows using Equation 11 as a starting point:

$$\boldsymbol{X}_{R2}^{h}(s,t)=\begin{bmatrix}\widetilde{\boldsymbol{r}_1}(s,t+2)\\ \widetilde{\boldsymbol{r}_1}(s+1,t+2)\\ .\\ .\\ .\\ \widetilde{\boldsymbol{r}_1}(s+M_r-2,t+2)\end{bmatrix}$$

$$.$$
$$.$$
$$.$$

$$\boldsymbol{X}_{RM_r}^{h}(s,t)=\widetilde{\boldsymbol{r}_1}(s,t+M_r)$$

$$\boldsymbol{X}_{R0}^{v}(s,t)=\begin{bmatrix}\widetilde{\boldsymbol{r}_2}(s,t)\\ \widetilde{\boldsymbol{r}_2}(s,t+1)\\ .\\ .\\ .\\ \widetilde{\boldsymbol{r}_2}(s,t+M_r)\end{bmatrix}$$

$$\boldsymbol{X}_{R}^{v}(s,t)=\begin{bmatrix}\boldsymbol{X}_{R0}^{v}(s,t)\\ \boldsymbol{X}_{R1}^{v}(s,t)\\ .\\ .\\ .\\ \boldsymbol{X}_{RM_r}^{v}(s,t)\end{bmatrix}$$

$$\boldsymbol{X}_{R1}^{v}(s,t)=\begin{bmatrix}\widetilde{\boldsymbol{r}_2}(s+1,t)\\ \widetilde{\boldsymbol{r}_2}(s+1,t+1)\\ .\\ .\\ .\\ \widetilde{\boldsymbol{r}_2}(s+1,t+M_r-1)\end{bmatrix}$$

$$\boldsymbol{X}_{R2}^{v}(s,t)=\begin{bmatrix}\widetilde{\boldsymbol{r}_2}(s+2,t)\\ \widetilde{\boldsymbol{r}_2}(s+2,t+1)\\ .\\ .\\ .\\ \widetilde{\boldsymbol{r}_2}(s+2,t+M_r-2)\end{bmatrix}$$

$$\boldsymbol{X}_{RM_r}^{v}(s,t)=\widetilde{\boldsymbol{r}_2}(s+M_r,t)$$

The above preview vector can be written as Equation 13.

$$\boldsymbol{X}_{RK}^{h}(s+1,t)=\boldsymbol{A}_{M_r-K}\boldsymbol{X}_{RK}^{h}(s,t)$$
$$\boldsymbol{X}_{RK}^{v}(s,t+1)=\boldsymbol{A}_{M_r-K}\boldsymbol{X}_{RK}^{v}(s,t) \tag{13}$$

$$\boldsymbol{X}_{R}^{\square}(s,t)=\begin{bmatrix}\boldsymbol{X}_{R0}^{h}(s,t)\\ \boldsymbol{X}_{R1}^{h}(s,t)\\ .\\ .\\ .\\ \boldsymbol{X}_{RM_r}^{\square}(s,t)\end{bmatrix}$$

The above preview vector can be written as Equation (14):

$$\boldsymbol{X}_{R}^{h}(s+1,t)=\boldsymbol{A}_{R}\boldsymbol{X}_{R}^{h}(s,t)$$
$$\boldsymbol{X}_{R}^{v}(s+1,t)=\boldsymbol{A}_{R}\boldsymbol{X}_{R}^{v}(s,t) \tag{14}$$

Where, $\boldsymbol{A}_R$ is defined as given below:

$$\boldsymbol{A}_R=\begin{bmatrix}0 & I & 0 & . & . & . & . & 0\\ 0 & 0 & I & 0 & . & . & . & 0\\ 0 & 0 & 0 & I & 0 & . & . & 0\\ . & . & . & . & . & . & . & .\\ . & . & . & . & . & . & . & .\\ . & . & . & . & . & . & . & .\\ 0 & 0 & 0 & 0 & 0 & . & . & I\\ 0 & 0 & 0 & 0 & 0 & . & . & 0\end{bmatrix}_{(M_r+1)p\times(M_r+1)p}$$

Where, $A_R=diag\left\{\boldsymbol{A}_{M_r}\quad \boldsymbol{A}_{M_r-1}\quad .\ .\ .\quad \boldsymbol{A}_0\right\}$

and

$$\boldsymbol{X}_{R}^{h}(s,t)\in(M_r+1)p,\quad \boldsymbol{X}_{R}^{v}(s,t)\in(M_r+1)p,\quad \boldsymbol{A}_R\in[(M_r+1)p\times(M_r+1)p],\ K=0,\ 1,\ 2\ldots M_r$$

The disturbance signal in horizontal direction is as follow:

$$\boldsymbol{X}_{w0}^{h}(s,t)=\begin{bmatrix}w_1(s,t)\\ w_1(s+1,t)\\ w_1(s+2,t)\\ .\\ .\\ .\\ w_1(s+M_d,t)\end{bmatrix}$$

$$\boldsymbol{X}_{w1}^{\square}(s,t)=\begin{bmatrix}w_1(s,t+1)\\ w_1(s+1,t+1)\\ w_1(s+2,t+1)\\ .\\ .\\ .\\ w_1(s+M_d-1,t+1)\end{bmatrix}$$

$$\boldsymbol{X}_{w2}^{\square}(s,t)=\begin{bmatrix}w_1(s,t+2)\\ w_1(s+1,t+2)\\ w_1(s+2,t+2)\\ .\\ .\\ .\\ w_1(s+M_d-2,t+2)\end{bmatrix}$$

$$.$$
$$.$$
$$.$$
$$.$$

$$\boldsymbol{X}_{wM_d}^{h}(s,t)=\begin{bmatrix}w_1(s,t+M_d)\\ w_1(s+1,t+M_d)\\ w_1(s+2,t+M_d)\\ .\\ .\\ .\\ w_1(s,t+M_d)\end{bmatrix}$$

Further, for the vertical direction, following are the disturbance signal:

$$\boldsymbol{X}_{w0}^{v}(s,t)=\begin{bmatrix} w_2(s,t)\\ w_2(s,t+1)\\ w_2(s,t+2)\\ .\\ .\\ .\\ w_2(s,t+M_d)\end{bmatrix}$$

$$\boldsymbol{X}_{w1}^{v}(s,t)=\begin{bmatrix} w_2(s+1,t)\\ w_2(s+1,t+1)\\ w_2(s+1,t+2)\\ .\\ .\\ .\\ w_2(s+1,t+M_d-1)\end{bmatrix}$$

$$\boldsymbol{X}_{w2}^{v}(s,t)=\begin{bmatrix} w_2(s+2,t)\\ w_2(s+2,t+1)\\ w_2(s+2,t+2)\\ .\\ .\\ .\\ w_2(s+2,t+M_d-2)\end{bmatrix}$$

$$\vdots$$

$$\boldsymbol{X}_{wM_d}^{v}(s,t)=\begin{bmatrix} w_2(s+M_d,t)\\ w_2(s+M_d,t+1)\\ w_2(s+M_d,t+2)\\ .\\ .\\ .\\ w_2(s+M_d,t)\end{bmatrix}$$

The above preview vector of disturbance can be written as Equation 15:

$$\begin{aligned}\boldsymbol{X}_{w}^{h}(s+1,t)&=\boldsymbol{A}_{w}\boldsymbol{X}_{w_1}^{h}(s,t)\\ \boldsymbol{X}_{w}^{v}(s,t+1)&=\boldsymbol{A}_{w}\boldsymbol{X}_{w_2}^{v}(s,t)\end{aligned} \tag{15}$$

where, $\boldsymbol{X}_{w_1}^{h}\in\boldsymbol{R}^{[(M_d+1)l]}$, $\boldsymbol{X}_{w_2}^{h}\in\boldsymbol{R}^{[(M_d+1)l]}$ and $\boldsymbol{A}_{w}\in\boldsymbol{R}^{[(M_d+1)l]\times[(M_d+1)l]}$

$$\boldsymbol{A}_w=\begin{bmatrix}0 & I & 0 & . & . & . & . & 0\\ 0 & 0 & I & 0 & . & . & . & 0\\ 0 & 0 & 0 & I & 0 & . & . & 0\\ . & . & . & . & . & . & . & .\\ . & . & . & . & . & . & . & .\\ . & . & . & . & . & . & . & .\\ 0 & 0 & 0 & 0 & 0 & . & . & I\\ 0 & 0 & 0 & 0 & 0 & . & . & 0\end{bmatrix}_{(M_d+1)l\times(M_d+1)l}$$

A preview-information-containing AE system must be created; the following augmented state vector can be defined as Equation 16:

$$\begin{cases}\widehat{\boldsymbol{x}}^{h}(s,t)=[\boldsymbol{e}_1{}^{T}(s,t)\quad \widetilde{\boldsymbol{x}}^{hT}(s,t)\quad \boldsymbol{X}_{R}^{h}{}^{T}(s,t)\quad \boldsymbol{X}_{W_1}^{h}{}^{T}(s,t)]^{T}\\ \widehat{\boldsymbol{x}}^{v}(s,t)=[\boldsymbol{e}_2{}^{T}(s,t)\quad \widetilde{\boldsymbol{x}}^{vT}(s,t)\quad \boldsymbol{X}_{R}^{v}{}^{T}(s,t)\quad \boldsymbol{X}_{W_2}^{v}{}^{T}(s,t)]^{T}\end{cases} \tag{16}$$

Creating the system in Equation 17 as follows:

$$\begin{cases}\widehat{\boldsymbol{x}}^{hT}(s+1,t)=\widehat{\boldsymbol{A}}_{11}\widehat{\boldsymbol{x}}^{h}(s,t)+\widehat{\boldsymbol{A}}_{12}\widehat{\boldsymbol{x}}^{v}(s,t)+\widehat{\boldsymbol{B}}_{1}\widetilde{\boldsymbol{u}}(s,t)\\ \widehat{\boldsymbol{x}}^{vT}(i,j+1)=\widehat{\boldsymbol{A}}_{21}\widehat{\boldsymbol{x}}^{h}(s,t)+\widehat{\boldsymbol{A}}_{22}\widehat{\boldsymbol{x}}^{v}(s,t)+\widehat{\boldsymbol{B}}_{2}\widetilde{\boldsymbol{u}}(s,t)\end{cases} \tag{17}$$

The constant matrix is shown in Equations 18 a–18 d. A summing operator that reduces static errors is absent from the closed-loop system. Therefore, by adding the integrator which is shown in Equation 19. From Equations 17 and 19, a new form of the system equation has been generated as Equation 20a to 20b.

$$\widehat{\boldsymbol{A}}_{11}=\begin{bmatrix}0 & \boldsymbol{C}_1A_{11} & \boldsymbol{G}_{PR} & \boldsymbol{G}_{PW_1}\\ 0 & \boldsymbol{A}_{11} & 0 & \boldsymbol{G}_{w_1}\\ 0 & 0 & \boldsymbol{A}_R & 0\\ 0 & 0 & 0 & \boldsymbol{A}_w\end{bmatrix},\quad \widehat{\boldsymbol{A}}_{12}=\begin{bmatrix}0 & \boldsymbol{C}_1\boldsymbol{A}_{12} & 0 & 0\\ 0 & \boldsymbol{A}_{12} & 0 & 0\\ 0 & 0 & 0 & 0\\ 0 & 0 & 0 & 0\end{bmatrix} \tag{18a}$$

$$\widehat{\boldsymbol{A}}_{21}=\begin{bmatrix}0 & C_2\boldsymbol{A}_{21} & 0 & 0\\ 0 & \boldsymbol{A}_{21} & 0 & 0\\ 0 & 0 & 0 & 0\\ 0 & 0 & 0 & 0\end{bmatrix},\quad \widehat{\boldsymbol{A}}_{22}=\begin{bmatrix}0 & C_2A_{22} & G_{PR} & G_{PW_2}\\ 0 & A_{22} & 0 & G_{w_2}\\ 0 & 0 & A_R & 0\\ 0 & 0 & 0 & \boldsymbol{A}_w\end{bmatrix} \tag{18b}$$

$$\widehat{\boldsymbol{B}}_1=\begin{bmatrix}\boldsymbol{C}_1\boldsymbol{B}_1\\ \boldsymbol{B}_1\\ 0\\ 0\end{bmatrix},\quad \widehat{\boldsymbol{B}}_2=\begin{bmatrix}\boldsymbol{C}_2\boldsymbol{B}_2\\ \boldsymbol{B}_2\\ 0\\ 0\end{bmatrix} \tag{18c}$$

$$\begin{cases} \boldsymbol{G}_{PR} = [0 \quad -\boldsymbol{I} \quad . \quad . \quad . \quad 0] \\ \boldsymbol{G}_{w1} = [\boldsymbol{E}_1 \quad 0 \quad . \quad . \quad . \quad 0] \\ \boldsymbol{G}_{w_2} = [\boldsymbol{E}_2 \quad 0 \quad . \quad . \quad . \quad 0] \\ \boldsymbol{G}_{Pw_1} = [\boldsymbol{C}_1\boldsymbol{E}_1 \quad 0 \quad . \quad . \quad . \quad 0] = \boldsymbol{C}_1\boldsymbol{G}_{w_1} \\ \boldsymbol{G}_{Pw_2} = [\boldsymbol{C}_2\boldsymbol{E}_2 \quad 0 \quad . \quad . \quad . \quad 0] = \boldsymbol{C}_2\boldsymbol{G}_{w_2} \end{cases} \tag{18d}$$

$$\begin{cases} V_1(s,t) = \sum_{k=0}^{s-1} e_1(k,t) + V_1(0,t) \\ V_2(s,t) = \sum_{k=0}^{t-1} e_2(s,k) + V_1(s,0) \end{cases} \tag{19}$$

$$\overline{\boldsymbol{x}}^h(s+1,t) = \begin{bmatrix} \widehat{\boldsymbol{A}}_{11} & 0 \\ \overline{\boldsymbol{C}} & \boldsymbol{I} \end{bmatrix} \begin{bmatrix} \widehat{\boldsymbol{x}}^h(s,t) \\ \boldsymbol{V}_1(s,t) \end{bmatrix} + \begin{bmatrix} \widehat{\boldsymbol{A}}_{12} & 0 \\ 0 & 0 \end{bmatrix} \begin{bmatrix} \widehat{\boldsymbol{x}}^v(s,t) \\ \boldsymbol{V}_2(s,t) \end{bmatrix} + \begin{bmatrix} \widehat{\boldsymbol{B}}_1 \\ 0 \end{bmatrix} \widetilde{\boldsymbol{u}}(s,t)$$

$$= \overline{\boldsymbol{A}}_{11}\overline{\boldsymbol{x}}^h(s,t) + \overline{\boldsymbol{A}}_{12}\overline{\boldsymbol{x}}^v(s,t) + \overline{\boldsymbol{B}}_1\widetilde{\boldsymbol{u}}(s,t) \tag{20a}$$

$$\overline{\boldsymbol{x}}^v(s,t+1) = \begin{bmatrix} \widehat{\boldsymbol{A}}_{21} & 0 \\ 0 & 0 \end{bmatrix} \begin{bmatrix} \widehat{\boldsymbol{x}}^h(s,t) \\ \boldsymbol{V}_1(s,t) \end{bmatrix} + \begin{bmatrix} \widehat{\boldsymbol{A}}_{22} & 0 \\ 0 & 0 \end{bmatrix} \begin{bmatrix} \widehat{\boldsymbol{x}}^v(s,t) \\ \boldsymbol{V}_2(s,t) \end{bmatrix} + \begin{bmatrix} \widehat{\boldsymbol{B}}_2 \\ 0 \end{bmatrix} \widetilde{\boldsymbol{u}}(s,t) \tag{20b}$$

$$= \overline{\boldsymbol{A}}_{21}\overline{\boldsymbol{x}}^{\square}(s,t) + \overline{\boldsymbol{A}}_{22}\overline{\boldsymbol{x}}^v(s,t) + \overline{\boldsymbol{B}}_2\widetilde{\boldsymbol{u}}(s,t)$$

Then the derived AE system is given as Equation 21:

$$\begin{bmatrix} \overline{\boldsymbol{x}}^h(s+1,t) \\ \overline{\boldsymbol{x}}^v(s,t+1) \end{bmatrix} = \begin{bmatrix} \overline{\boldsymbol{A}}_{11} & \overline{\boldsymbol{A}}_{12} \\ \overline{\boldsymbol{A}}_{21} & \overline{\boldsymbol{A}}_{22} \end{bmatrix} \begin{bmatrix} \overline{\boldsymbol{x}}^h(s,t) \\ \overline{\boldsymbol{x}}^v(s,t) \end{bmatrix} + \begin{bmatrix} \overline{\boldsymbol{B}}_1 \\ \overline{\boldsymbol{B}}_2 \end{bmatrix} \boldsymbol{u}(s,t) \tag{21}$$

Good tracking performance must be attained, robustness to disturbances, and optimal control, the control law can be designed using the AE system, which is a difference equation.

### 3.4Preview controller design

Using a model of the system being controlled to predict its future behavior and using that prediction to change the control inputs in real time, is known as "preview control".

In preview control, by predicting disruptions or other changes in the system and making adjustments for them, the control system's performance is improved. In the following paragraphs, the detailed steps of preview controller design is discussed. For the AE system Equation 21, the input vector is given as Equation 22:

$$\boldsymbol{u}(s,t) = \begin{bmatrix} \boldsymbol{K}_1 & \boldsymbol{K}_2 \end{bmatrix} \begin{bmatrix} \overline{\boldsymbol{x}}^h(s,t) \\ \overline{\boldsymbol{x}}^v(s,t) \end{bmatrix}$$

$$= \boldsymbol{K}_1\overline{\boldsymbol{x}}^h(s,t) + \boldsymbol{K}_2\overline{\boldsymbol{x}}^v(s,t) \tag{22}$$

where $\boldsymbol{K}_1$ and $\boldsymbol{K}_2$ are gain matrix. Hence, by using Equation 22, the derived closed-loop system is given below in Equation 23:

$$\begin{bmatrix} \overline{\boldsymbol{x}}^h(s+1,t) \\ \overline{\boldsymbol{x}}^v(s,t+1) \end{bmatrix} = \begin{bmatrix} \overline{\boldsymbol{A}}_{11} + \overline{\boldsymbol{B}}_1\boldsymbol{K}_1 & \overline{\boldsymbol{A}}_{12} + \overline{\boldsymbol{B}}_1\boldsymbol{K}_2 \\ \overline{\boldsymbol{A}}_{21} + \overline{\boldsymbol{B}}_2\boldsymbol{K}_1 & \overline{\boldsymbol{A}}_{22} + \overline{\boldsymbol{B}}_2\boldsymbol{K}_2 \end{bmatrix} \begin{bmatrix} \overline{\boldsymbol{x}}^h(s,t) \\ \overline{\boldsymbol{x}}^v(s,t) \end{bmatrix} \tag{23}$$

Asymptotic stability was achieved for the closed-loop system in Equation 23 by the proposed state feedback controller (Equation 22), as shown in Equation 24:

$$\begin{cases} \lim\limits_{s+t\to\infty} \overline{x}^h(s,t) = 0 \\ \lim\limits_{s+t\to\infty} \overline{x}^v(s,t) = 0 \end{cases} \tag{24}$$

Since $\boldsymbol{e}_1(s,t)$ is a part of $\overline{\boldsymbol{x}}^h(s,t)$ and $\boldsymbol{e}_2(s,t)$ is a part of $\overline{\boldsymbol{x}}^v(s,t)$, Equations 25a-25b show the error values as time goes towards the infinity.

$$\lim_{s+t\to\infty} \boldsymbol{e}_1(s,t) = \boldsymbol{0}, \qquad \lim_{s+t\to\infty} \boldsymbol{e}_2(s,t) = \boldsymbol{0} \tag{25a}$$

$$\lim_{s+t\to\infty} \boldsymbol{e}(s,t) = \lim_{s+t\to\infty} [\boldsymbol{e}_1(s,t) + \boldsymbol{e}_2(s,t)] = \boldsymbol{0} \tag{25b}$$

It was seen that the designed controller which included the reference signal's preview behavior could realize the accurate tracking of the reference signal by the output of the system 1a-1b under state feedback. A necessary condition for the closed-loop system in Equation 23 to be asymptotically stable, was provided by Theorem 1.

**Theorem 1:** The closed-loop system in Equation 23 is asymptotically stable, if there exist positive definite symmetric matrices $\boldsymbol{X}_1, \boldsymbol{X}_2$ and $\boldsymbol{Y}_1, \boldsymbol{Y}_2$ satisfying the following inequality shown in Equation 26.

$$\boldsymbol{\gamma} = \begin{bmatrix} -\boldsymbol{X}_1 & \boldsymbol{0} & \bar{\boldsymbol{A}}_{11}\boldsymbol{X}_1 + \bar{\boldsymbol{B}}_1\boldsymbol{Y}_2 & \bar{\boldsymbol{A}}_{12}\boldsymbol{X}_2 + \bar{\boldsymbol{B}}_1\boldsymbol{Y}_2 \\ \boldsymbol{0} & -\boldsymbol{X}_2 & \bar{\boldsymbol{A}}_{21}\boldsymbol{X}_1 + \bar{\boldsymbol{B}}_2\boldsymbol{Y}_1 & \bar{\boldsymbol{A}}_{22}\boldsymbol{X}_2 + \bar{\boldsymbol{B}}_2\boldsymbol{Y}_2 \\ * & * & -\boldsymbol{X}_1 & \boldsymbol{0} \\ * & * & * & -\boldsymbol{X}_2 \end{bmatrix} < \boldsymbol{0} \tag{26}$$

**Proof:** Let define a Lyapunov function as follows.

$$\mathrm{V}(s,t) = \mathrm{V}(\bar{\boldsymbol{x}}^h(s,t)) + \mathrm{V}(\bar{\boldsymbol{x}}^v(s,t))$$
$$= \bar{\boldsymbol{x}}^{hT}(s,t)\boldsymbol{P}_h\bar{\boldsymbol{x}}^h(s,t) + \bar{\boldsymbol{x}}^{vT}(s,t)\boldsymbol{P}_v\bar{\boldsymbol{x}}^v(s,t)$$

where $P_h$ and $P_v$ are positive semi-definite matrices. The difference of the above Lyapunov function is given by Equation 27.

$$\Delta\mathrm{V}(s,t) = [\mathrm{V}(\bar{\boldsymbol{x}}^h(s+1,t)) + \mathrm{V}(\bar{\boldsymbol{x}}^v(s,t+1))] - [\mathrm{V}(\bar{\boldsymbol{x}}^h(s,t)) + \mathrm{V}(\bar{\boldsymbol{x}}^v(s,t))]$$
$$= \begin{bmatrix} \bar{\boldsymbol{x}}^{hT}(s,t) \\ \bar{\boldsymbol{x}}^{vT}(s,t) \end{bmatrix}^T \boldsymbol{\Omega} \begin{bmatrix} \bar{\boldsymbol{x}}^h(s,t) \\ \bar{\boldsymbol{x}}^v(s,t) \end{bmatrix} \tag{27}$$

Where,

$$\boldsymbol{\Omega} = \begin{bmatrix} (\bar{\boldsymbol{A}}_{11} + \bar{\boldsymbol{B}}_1\boldsymbol{K}_1)^T\boldsymbol{P}_h(\bar{\boldsymbol{A}}_{11} + \bar{\boldsymbol{B}}_1\boldsymbol{K}_1)^T + (\bar{\boldsymbol{A}}_{21} + \bar{\boldsymbol{B}}_2\boldsymbol{K}_1)^T\boldsymbol{P}_v(\bar{\boldsymbol{A}}_{21} + \bar{\boldsymbol{B}}_2\boldsymbol{K}_2) & (\bar{\boldsymbol{A}}_{11} + \bar{\boldsymbol{B}}_1\boldsymbol{K}_1)^T\boldsymbol{P}_h(\bar{\boldsymbol{A}}_{11} + \bar{\boldsymbol{B}}_1\boldsymbol{K}_2)^T + (\bar{\boldsymbol{A}}_{21} + \bar{\boldsymbol{B}}_2\boldsymbol{K}_1)^T\boldsymbol{P}_v(\bar{\boldsymbol{A}}_{22} + \bar{\boldsymbol{B}}_2\boldsymbol{K}_2) \\ (\bar{\boldsymbol{A}}_{12} + \bar{\boldsymbol{B}}_1\boldsymbol{K}_2)^T\boldsymbol{P}_h(\bar{\boldsymbol{A}}_{22} + \bar{\boldsymbol{B}}_2\boldsymbol{K}_2)^T + (\bar{\boldsymbol{A}}_{22} + \bar{\boldsymbol{B}}_2\boldsymbol{K}_2)^T\boldsymbol{P}_v(\bar{\boldsymbol{A}}_{21} + \bar{\boldsymbol{B}}_2\boldsymbol{K}_2) & (\bar{\boldsymbol{A}}_{12} + \bar{\boldsymbol{B}}_1\boldsymbol{K}_2)^T\boldsymbol{P}_h(\bar{\boldsymbol{A}}_{12} + \bar{\boldsymbol{B}}_1\boldsymbol{K}_2)^T + (\bar{\boldsymbol{A}}_{22} + \bar{\boldsymbol{B}}_2\boldsymbol{K}_2)^T\boldsymbol{P}_v(\bar{\boldsymbol{A}}_{22} + \bar{\boldsymbol{B}}_2\boldsymbol{K}_2) \end{bmatrix}$$

Taking the positive definite matrices mentioned in Theorem 1 as $\boldsymbol{X}_1 = \boldsymbol{P}_h^{-1}$, $\boldsymbol{X}_2 = \boldsymbol{P}_v^{-1}$, $\boldsymbol{Y}_1 = \boldsymbol{K}_1\boldsymbol{X}_1$, $\boldsymbol{Y}_2 = \boldsymbol{K}_2\boldsymbol{X}_2$.

By substituting the values of the matrices $\boldsymbol{X}_1, \boldsymbol{X}_2$ and $\boldsymbol{Y}_1, \boldsymbol{Y}_2$ in Equation 26, we got the following Equation 28.

$$\begin{bmatrix} -\boldsymbol{P}_h^{-1} & \boldsymbol{0} & \bar{\boldsymbol{A}}_{11} + \bar{\boldsymbol{B}}_1\boldsymbol{K}_1 & \bar{\boldsymbol{A}}_{12} + \bar{\boldsymbol{B}}_1\boldsymbol{K}_2 \\ \boldsymbol{0} & -\boldsymbol{P}_v^{-1} & \bar{\boldsymbol{A}}_{21} + \bar{\boldsymbol{B}}_2\boldsymbol{K}_1 & \bar{\boldsymbol{A}}_{22} + \bar{\boldsymbol{B}}_2\boldsymbol{K}_2 \\ * & * & -\boldsymbol{P}_h & \boldsymbol{0} \\ * & * & * & -\boldsymbol{0}_v \end{bmatrix} = \boldsymbol{Q}^T\boldsymbol{\gamma}\,\boldsymbol{Q} < \boldsymbol{0} \tag{28}$$

In the above Equation, $\boldsymbol{Q} = diag\{\boldsymbol{I} \quad \boldsymbol{I} \quad \boldsymbol{P_h} \quad \boldsymbol{P_v}\}$.

Using Schur complement lemma [14], $\boldsymbol{\Omega} < \boldsymbol{0}$, which led to $\Delta\mathrm{V}(s,t) \le 0$.

If and only if at that time the equal sign was established, then

$$\begin{bmatrix} \bar{\boldsymbol{x}}^{hT}(s,t) & \bar{\boldsymbol{x}}^{vT}(s,t) \end{bmatrix}^T = \boldsymbol{0}$$

Equation 29 was designed with the help of Lyapunov theory to establish the stability

$$\mathrm{V}(\bar{\boldsymbol{x}}^h(s+1,t)) + \mathrm{V}(\bar{\boldsymbol{x}}^v(s,t+1)) \le \mathrm{V}(\bar{\boldsymbol{x}}^h(s,t)) + \mathrm{V}(\bar{\boldsymbol{x}}^v(s,t)) \tag{29}$$

Define the set $D(r) \triangleq \{(s,t): s+t=r, \quad s \ge 0, t \ge 0\}$

$$\sum_{s+t\in D(r)} \left[\mathrm{V}(\bar{\boldsymbol{x}}^h(s,t)) + \mathrm{V}(\bar{\boldsymbol{x}}^v(s,t))\right] =$$

Based on the boundary conditions given in this paper, from Equation 21, we obtained

$$\mathrm{V}(\bar{x}^h(0,r)) + \mathrm{V}((\bar{x}^h(1,r-1)) + \ldots + \mathrm{V}(\bar{x}^h(r-1,1)) + \mathrm{V}(\bar{x}^h(r,0))$$
$$\mathrm{V}(\bar{x}^v(r,0)) + \mathrm{V}(\bar{x}^v(r-1,1)) + \ldots + \mathrm{V}(\bar{x}^v(r-1,1)) + \mathrm{V}(\bar{x}^v(1,r-1)) + \mathrm{V}(\bar{x}^v(0,r))$$
$$\geq \mathrm{V}(\bar{x}^h(1,r)) + \mathrm{V}(\bar{x}^h(2,r-1)) + \ldots + \mathrm{V}(\bar{x}^h(r,1)) + \mathrm{V}(\bar{x}^h(r+1,0)) +$$
$$\mathrm{V}(\bar{x}^v(r,1)) + \mathrm{V}(\bar{x}^v(r-1,2)) + \ldots + \mathrm{V}(\bar{x}^v(1,r)) + \mathrm{V}(\bar{x}^v(0,r+1))$$
$$= \mathrm{V}(\bar{x}^h(0,r+1)) + \mathrm{V}(\bar{x}^h(1,r)) + \ldots + \mathrm{V}(\bar{x}^h(r,1)) + \mathrm{V}(\bar{x}^h(r+1,0)) +$$
$$\mathrm{V}(\bar{x}^v(r+1,0)) + \mathrm{V}(\bar{x}^v(r,1)) + \ldots + \mathrm{V}(\bar{x}^v(1,r)) + \mathrm{V}(\bar{x}^v(0,r+1))$$
$$= \sum_{s+t\in D(r+1)} [\mathrm{V}(\bar{x}^h(s,t)) + \mathrm{V}(\bar{x}^v(s,t))]$$

i.e. $\sum_{s+t\in D(r+1)} V(s,t) \leq \sum_{s+t\in D(r)} V(s,t)$

To get $\lim\limits_{r\to\infty} \sum_{s+t\in D(r)} \mathrm{V}(s,t) = 0$ So, $\lim\limits_{s+t\to\infty} \mathrm{V}(s,t) = 0$, $\lim\limits_{s+t\to\infty} \|x(s,t)\| = \mathbf{0}$

Hence, the closed-loop system's asymptotic stability was proved.

**Note 1:** Theorem 1 demonstrated that there was state feedback in the AE system for the closed-loop system that was asymptotically stable if LMI in Equation 26 had a set of feasible solutions. The system's horizontal state is indicated as follows in Equation 30a:

$$\begin{aligned}\bar{\boldsymbol{x}}^h(s,t) = [&e_1{}^T(s,t) \quad \tilde{\boldsymbol{x}}^{h^T}(s,t) \quad \tilde{r}_1{}^T(s,t) \quad \tilde{r}_1{}^T(s+1,t) \quad \ldots \quad \tilde{r}_1{}^T(s+M_r,t) \\ &\tilde{r}_1{}^T(s,t+1) \quad \tilde{r}_1{}^T(s+1,t+1) \quad \tilde{r}_1{}^T(s+2,t+1) \quad \ldots \quad \tilde{r}_1{}^T(s+M_r-1,t+1)\ldots\tilde{r}_1{}^T(s,t+M_r) \\ &w_1{}^T(s,t) \quad w_1{}^T(s+1,t) \quad w_1{}^T(s+1,t) \ldots \quad w_1{}^T(s+M_d,t) \\ &w_1{}^T(s,t+1) \quad w_1{}^T(s,t+1) \quad w_1{}^T(s,t+2) \quad \ldots \quad w_1{}^T(s,t+M_d) \quad V_1(s,t)]^T\end{aligned} \tag{30a}$$

The system's vertical state is indicated as follows in Equation 30 b

$$\begin{aligned}\bar{\boldsymbol{x}}^v(s,t) = [&e_2{}^T(s,t) \quad \tilde{\boldsymbol{x}}^{v^T}(s,t) \quad \tilde{r}_2{}^T(s,t) \quad \tilde{r}_2{}^T(s,t+1) \quad \ldots \quad \tilde{r}_2{}^T(s,t+M_r) \\ &\tilde{r}_2{}^T(s+1,t) \quad \tilde{r}_2{}^T(s+1,t+1) \quad \tilde{r}_2{}^T(s+1,t+2) \quad \ldots \quad \tilde{r}_2{}^T(s+1,t+M_r-1)\ldots \\ &\tilde{r}_2{}^T(s+M_r,t) \quad w_2{}^T(s,t) \quad w_2{}^T(s,t+1) \quad w_2{}^T(s,t+2) \ldots \quad w_2{}^T(s,t+M_d) \\ &w_2{}^T(s,t+1) \quad w_2{}^T(s,t+1) \quad w_2{}^T(s,t+2) \quad \ldots \quad w_2{}^T(s,t+M_d) \ldots w_2{}^T(s+M_d,t) \quad V_2(s,t)]^T\end{aligned} \tag{30b}$$

Therefore, the gain matrix could be decomposed into the following Equation 31. Then the designed preview controller is given by Equation 32. **Theorem 2:** Assuming that Assumptions 1-3 are satisfied and if the LMI in Equation 26 has feasible solution, then the expression of the designed system controller is given in Equation 33.

$$\begin{aligned}K = [K_1 \quad K_2] = \Big[&K_{e1} \quad K_{\hat{x}_h} \quad K_{r_1}(0,0) \quad K_{r_1}(1,0) \quad \ldots \quad K_{r_1}(M_r,0) \quad K_{r_1}(0,1) \quad K_{r_1}(1,1) \quad \ldots \\ &K_{r_1}(M_{r-1},1) \quad K_{r_1}(0,M_r) \quad \ldots \quad K_{w_1}(0,0) \quad K_{w_1}(1,0) \quad K_{w_1}(0,M_d) \ldots K_{v1} \quad K_{e2} \quad K_{\hat{x}v} \quad K_{r_2}(0,0) \quad K_{r_2}(0,1) \quad \ldots \quad K_{r_2}(1,0) \quad K_{r_2}(0,M_r) \\ &K_{r2}(1,1) \quad K_{r2}(1,M_r-1) \quad \ldots \quad K_{r2}(M_r,0) \quad K_{w_2}(0,0) \quad K_{w_2}(0,1) \quad \ldots K_{w_2}(0,M_d) \quad K_{v_2}\Big]\end{aligned} \tag{31}$$

$$\begin{aligned}\boldsymbol{u}(s,t) = &K_{e1}\, e_1(s,t) + K_{x_h}\, x^h(s,t) + \sum_{l=0}^{M_r} \sum_{m=0}^{M_r} K_{r1}(s,t)\, r_1(s+m,t+l) + \\ &\sum_{l=0}^{M_d} \sum_{m=0}^{M_d} K_{w_1}(l,m)\, w_1(s+m,t+l) + K_{v_1} V_1(s,t) + K_{e2}\, e_2(s,t) + K_{x_h}\, x^v(s,t) + \\ &\sum_{l=0}^{M_r} \sum_{m=0}^{M_r} K_{r_2}(l,m)\, r_2(s+m,t+l) + \sum_{l=0}^{M_d} \sum_{m=0}^{M_d} K_{w_2}(l,m)\, w_2(s+m,t+l) + K_{v_2} V_2(s,t)\end{aligned} \tag{32}$$

$$u(s,t)=K_{e1}\,e_1(s,t)+K_{x_h}\,x^h(s,t)+\sum_{l=0}^{M_r}\sum_{m=0}^{M_r}K_{r1}(l,m)r_1(s+m,t+l)-\sum_{l=0}^{M_r}\sum_{m=0}^{M_r}K_{r1}(l,m)*r_1^*+$$
$$\sum_{l=0}^{M_d}\sum_{m=0}^{M_d}K_{w_1}(l,m)\,w_1(s+m,t+l)+K_{v_1}(\sum_{k=0}^{s-1}e_2(k,t)+V_1(0,t))+K_{e2}\,e_2(s,t)+K_{x_v}\,x^v(s,t)+$$
$$\sum_{l=0}^{M_r}\sum_{m=0}^{M_r}K_{r_2}(l,m)r_2(s+m,t+l)-\sum_{l=0}^{M_r}\sum_{m=0}^{M_r}K_{r_2}(l,m)r_2^*+$$
$$+\sum_{l=0}^{M_d}\sum_{m=0}^{M_d}K_{w_2}(l,m)\,w_2(s+m,t+l)+K_{v2}(\sum_{k=0}^{t-1}e_2(s,k)+V_2(s,0))-\begin{bmatrix}K_{x_h} & K_{x_v} & -I\end{bmatrix}\begin{bmatrix}x_h^*\\x_v^*\\u^*\end{bmatrix} \tag{33}$$

Proof of Equation 33:
Based on Theorem 1, the controller gain matrix $(\boldsymbol{K}_i=\boldsymbol{X}_i^{-1}\boldsymbol{Y}_i)$ can be obtained by solving the LMI in Equation 26, where $\boldsymbol{X}_i(i=1,2)$ and $\boldsymbol{Y}_i(i=1,2)$ are the positive definite symmetric matrices. Using Equation 22, we obtain Equation 34. Using Equation 10 and Equation 34 the controller can be formed as Equation 35:
**Note 2:** It may be noted that the expected preview controller can be obtained by using the preview controller $\boldsymbol{u}(s,t)$ given in Equation 22 and original system controller $u(s,t)$ given in Equation in 35.

By using Equation 36, we obtained original controller given in Equation 33.
**Note 3:** The matrix $\boldsymbol{X}_i$ and the invertible matrix $\boldsymbol{Y}_i$ were determined by the Equation 26 for $(i=1,2)$.
Equation 31 determined the gain matrix variables. Further, using Equation 33, it was shown that Equation 26 ensured the asymptotic stability of the closed loop system.

$$\boldsymbol{u}(s,t)=K_1\bar{\boldsymbol{x}}^h(s,t)+K_2\bar{\boldsymbol{x}}^v(s,t)$$
$$=K_{e_1}\,e_1(s,t)+K_{x_h}\,x^h(s,t)+\sum_{l=0}^{M_r}\sum_{m=0}^{M_r}K_{r1}(l,m)\,r_1(s+m,t+l)+$$
$$\sum_{l=0}^{M_d}\sum_{m=0}^{M_d}K_{w_1}(l,m)\,w_1(s+m,t+l)+K_{v_1}V_1(s,t)+K_{e2}\,e_2(s,t)+K_{x_v}\,x^v(s,t)+$$
$$\sum_{l=0}^{M_r}\sum_{m=0}^{M_r}K_{r_2}(l,m)\,r_2(s+m,t+l)+\sum_{l=0}^{M_d}\sum_{m=0}^{M_d}K_{w_1}(l,m)\,w_2(s+m,t+l)+K_{v_2}V_2(s,t) \tag{34}$$

Where,

$$\boldsymbol{K}=\begin{bmatrix}\boldsymbol{K}_1 & \boldsymbol{K}_2\end{bmatrix}=\Big[K_{e1}\quad K_{x_h}\quad K_{r_1}(0,0)\quad K_{r_1}(1,0)\quad \ldots\quad K_{r_1}(M_r,0)\quad K_{r_1}(0,1)\quad K_{r_1}(1,1)\quad \ldots$$
$$K_{r_1}(M_{r-1},1)\quad K_{r_1}(0,M_r)\quad K_{w_1}(0,0)\quad K_{w_1}(1,0)\ldots K_{w_1}(M_d,0)\quad K_{v_1}\quad K_{e_2}\quad K_{x_v}\quad K_{r_2}(0,0)\quad K_{r_2}(0,1)\quad \ldots\quad K_{r_2}(1,0)\quad K_{r_2}(0,M_r)$$
$$K_{r_2}(1,1)\quad K_{r_2}(1,M_r-1)\quad \ldots\quad K_{r_2}(M_r,0)\quad K_{w_2}(0,0)\quad K_{w_2}(0,1)\quad \ldots K_{w_2}(0,1)\quad \ldots\quad K_{w_2}(1,0)\quad K_{w_2}(0,M_d)\quad K_{v_2}\Big]$$

$$u(s,t)=K_{e_1}\,e_1(s,t)+K_{x_h}\,x^h(s,t)+\sum_{l=0}^{M_r}\sum_{m=0}^{M_r}K_{r_1}(l,m)\,r_1(l+m,t+l)-\sum_{l=0}^{M_r}\sum_{m=0}^{M_r}K_{r_1}(l,m)*r_1^*+$$
$$\sum_{l=0}^{M_d}\sum_{m=0}^{M_d}K_{w_1}(l,m)\,w_1(l+m,t+l)+K_{v_1}(\sum_{k=0}^{s-1}e_2(k,t)+V_1(0,t))+K_{e_2}\,e_2(s,t)+K_{x_v}\,x^v(s,t)+$$
$$\sum_{l=0}^{M_r}\sum_{m=0}^{M_r}K_{r_2}(l,m)\,r_2(l+m,t+l)-\sum_{l=0}^{M_r}\sum_{m=0}^{M_r}K_{r_2}(l,m)\,r_2^*$$
$$+\sum_{l=0}^{M_d}\sum_{m=0}^{M_d}K_{w_2}(l,m)\,w_2(l+m,t+l)+K_{v_2}(\sum_{k=0}^{t-1}e_2(s,k)+V_2(s,0))-\begin{bmatrix}K_{\widehat{xh}} & K_{\widehat{xv}} & -I\end{bmatrix}\begin{bmatrix}x_h^*\\x_v^*\\u^*\end{bmatrix} \tag{35}$$

Using Equation 10, we obtained the Equation 36.

$$x^h(s,t)=\tilde{x}^h(s,t)+x_h^*$$
$$x^v(s,t)=\tilde{x}^v(s,t)+x_h^*$$
$$u(s,t)=\tilde{u}(s,t)+x_h^*$$
$$r_1(s,t)=\tilde{r}_1(s,t)+r_1{}^*$$
$$r_2(s,t)=\tilde{r}_2(s,t)+r_2{}^* \tag{36}$$

## 4. Results

To check the effectiveness of the proposed algorithm, consider that the required parameters in Equation 1a–1c are given in the following example.

**Example:** Consider an example of Rosser model for 2-D DT systems.

$A_{11} = -2.1, \quad A_{12} = 0.5, \quad A_{21} = 1.5, \quad A_{22} = 2.5$

$B_1 = -0.2, \quad B_2 = 1.5,$

$C_1 = 2.5, \quad C_2 = 10$

$E_1 = 0.3, \quad E_2 = 0$

Take the reference signal $r(s,t) = r_1(s,t) + r_2(s,t) = 1$. In order to satisfy the rank condition of Assumption 3, we might take $r_1(s,t) = 0$ and $r_2(s,t) = 1$. The Equation 9 was solved to obtain $x_h^* = 0$, $x_v^* = 0.1$, $u^* = 0.25$ by considering the boundary conditions $\boldsymbol{x}^h(0,t) = \boldsymbol{x}^v(s,0) = 0$, and the initial conditions $V_1(0,t) = V_2(s,0) = 0$. Based on Theorem 2, the matrix variables $\boldsymbol{X}_1, \boldsymbol{X}_2$ and $\boldsymbol{Y}_1, \boldsymbol{Y}_2$ were obtained by solving LMI in Equation 26, and hence, required gain matrix was achieved as $\boldsymbol{K}_i = \boldsymbol{X}_i^{-1}\boldsymbol{Y}_i, \quad (i = 1, 2)$.

If $M_r = 0$, then

$$K_1 = \begin{bmatrix} K_{e_1} & K_{\hat{x}_h} & K_{r_1}(0,0) & K_{d_1}(0,0) & K_{v_1} \end{bmatrix}$$

$$K_1 = \begin{bmatrix} K_{e_1} & K_{\hat{x}_h} & K_{r_1}(0,0) & K_{d_1}(0,0) & K_{v_1} \end{bmatrix}$$

$$K_1 = \begin{bmatrix} 0.0001 & -1.0012 & 0 & 0.0002 & 0.0003 \end{bmatrix}$$

$$K_2 = \begin{bmatrix} K_{e_2} & K_{x_h} & K_{r_2}(0,0) & K_{d_2}(0,0) & K_{v_2} \end{bmatrix}$$

$$K_2 = \begin{bmatrix} -0.0013 & -1.2020 & 0 & 0.0001 & -0.0322 \end{bmatrix}$$

If $M_r = 2$, then

$$K_1 = \Big[ K_{e_1} \quad K_{x_h} \quad K_{r_1}(0,0) \quad K_{r_1}(1,0) \quad K_{r_1}(2,0) \quad K_{r_1}(0,1) \quad K_{r_1}(1,1) \quad K_{r_1}(0,2)$$
$$K_{d_1}(0,0) \quad K_{d_1}(1,0) \quad K_{d_1}(2,0) \quad K_{d_1}(0,1) \quad K_{d_1}(1,1) \quad K_{d_1}(0,2) \quad K_{v_1} \Big]$$

$$K_1 = \big[ 0.0004 \quad -1.0029 \quad -0.0000 \quad -0.0083 \quad -0.0005 \quad -0.0000 \quad -0.0000 \quad -0.0000$$
$$0.004 \quad -0.0002 \quad 0.0001 \quad -0.0000 \quad 0.0000 \quad -0.0000 \quad 0.0045 \big]$$

$$K_2 = \Big[ K_{e_2} \quad K_{x_v} \quad K_{r_2}(0,0) \quad K_{r_2}(1,0) \quad K_{r_2}(2,0) \quad K_{r_2}(0,1) \quad K_{r_2}(1,1) \quad K_{r_2}(0,2)$$
$$K_{d_2}(0,0) \quad K_{d_2}(1,0) \quad K_{d_2}(2,0) \quad K_{d_2}(0,1) \quad K_{d_2}(1,1) \quad K_{d_2}(0,2) \quad K_{v_2} \Big]$$

$$K_2 = \big[ -0.0053 \quad -1.2547 \quad -0.0000 \quad 0.0061 \quad 0.0502 \quad 0.0000 \quad 0.0000 \quad 0.0000$$
$$0.0001 \quad -0.0001 \quad -0.0001 \quad -0.0000 \quad -0.0000 \quad -0.0000 \quad -0.0023 \big]$$

If $M_r = 4$, then

$$K_1 = \Big[ K_{e_1} \quad K_{x_h} \quad K_{r_1}(0,0) \quad K_{r_1}(1,0) \quad K_{r_1}(2,0) \quad K_{r_1}(3,0) \quad K_{r_1}(4,0) \quad K_{r_1}(0,1)$$
$$K_{r_1}(1,1) \quad K_{r_1}(0,3) \quad K_{r_1}(0,4) \quad K_{d_1}(0,0) \quad K_{d_1}(1,0) \quad K_{d_1}(2,0) \quad K_{d_1}(3,0) \quad K_{d_1}(4,0)$$
$$K_{d_1}(0,1) \quad K_{d_1}(0,2) \quad K_{d_1}(0,3) \quad K_{d_1}(0,4) \quad K_{v_1} \Big]$$

$$K_2 = \Big[ K_{e_2} \quad K_{x_v} \quad K_{r_2}(0,0) \quad K_{r_2}(0,1) \quad K_{r_2}(0,2) \quad K_{r_2}(0,3) \quad K_{r_2}(0,4) \quad K_{r_2}(1,0)$$
$$K_{r_2}(1,1) \quad K_{r_2}(1,2) \quad K_{r_2}(1,3) \quad K_{r_2}(2,0) \quad K_{r_2}(2,1) \quad K_{r_2}(3,2) \quad K_{r_2}(3,0) \quad K_{r_2}(3,1)$$
$$K_{r_2}(4,0) \quad K_{d_2}(0,0) \quad K_{d_2}(0,1) \quad K_{d_2}(0,2) \quad K_{d_2}(0,3) \quad K_{d_2}(0,4) \quad K_{d_2}(1,0) \quad K_{d_2}(1,1)$$
$$K_{d_2}(1,2) \quad K_{d_2}(1,3) \quad K_{d_2}(2,0) \quad K_{d_2}(2,1) \quad K_{d_2}(3,2) \quad K_{d_2}(3,0) \quad K_{d_2}(3,1) \quad K_{d_2}(4,0) \quad K_{v_2} \Big]$$

With the help of YALMIP toolbox, the value of $t_{min}$ was negative which indicated a feasible solution.

Assuming that the boundary condition $x^h(0,t) = x^v(s,0) = 0$ and the initial condition $V_1(0,t) = V_2(s,0) = 0$, these simulation results are displayed. The open loop system's horizontal and vertical states are depicted in *Figures 2 and 3*, respectively.

By the analysis of *Figures 2 and 3*, it was observed that the open loop systems were unstable for both horizontal state as well as vertical states. The closed-loop system's horizontal and vertical states are depicted in *Figures 4* and *5*, respectively. *Figures 4* and *5* shows that the closed-loop systems are stable for both horizontal state as well as vertical states by using the proposed control law. *Figures 6* and *7* show the horizontal and vertical tracking error of the closed-loop system tend to zero when simulated for preview length $M_r = 2$.

In order to compare with the tracking error plots (*Figures 6* and *7*) for preview length $M_r = 2$, we had also plotted the tracking error plots (*Figures 8* and *9*) for preview length $M_r = 0$. It was observed that the tracking error plots obtained without preview length ($M_r$=0) had large tracking error initially as compared to the tracking error plots obtained with preview length ($M_r$=2).

**Error impacts:** It was noteworthy that the overall error clearly impacted the system state response. In the *Figures 6* and *7*, errors increase initially and due to this, the augmented system states also show reasonable variation (*Figures 4* and *5*). However, as soon as the proposed preview controller was applied to the system, the errors decreased towards origin. This decrement in the error directly impacted the system states and led them to the origin as well, depicted in *Figures 4* and *5*. When a value of preview length is taken as zero, then *Figures 8* and *9* show the error in the horizontal and vertical directions.

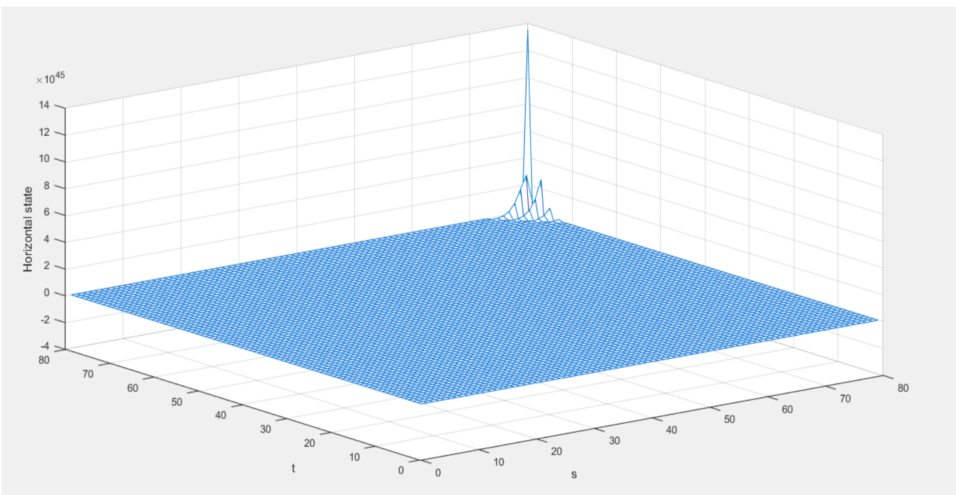


**Figure 2** Horizontal state of open loop system

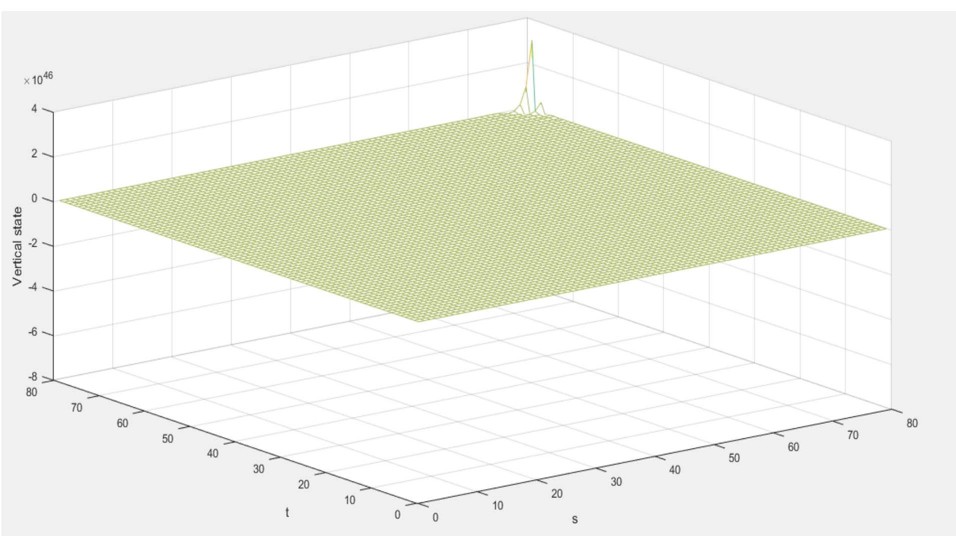


**Figure 3** Vertical state of open loop system

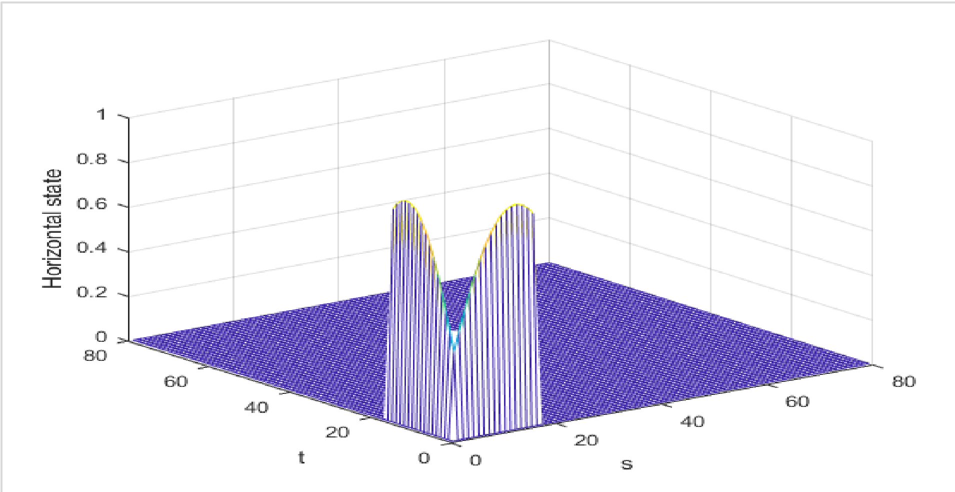


**Figure 4** Horizontal state of closed loop system

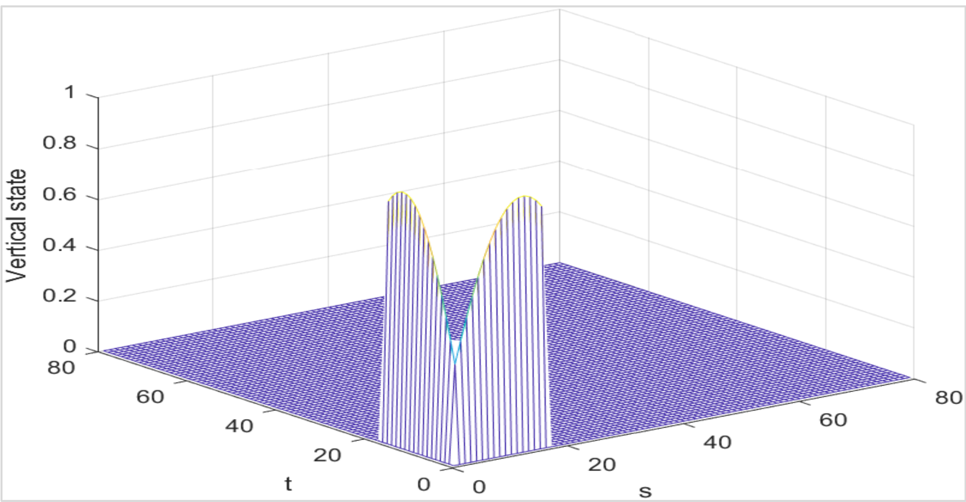


**Figure 5** Vertical state of closed loop system

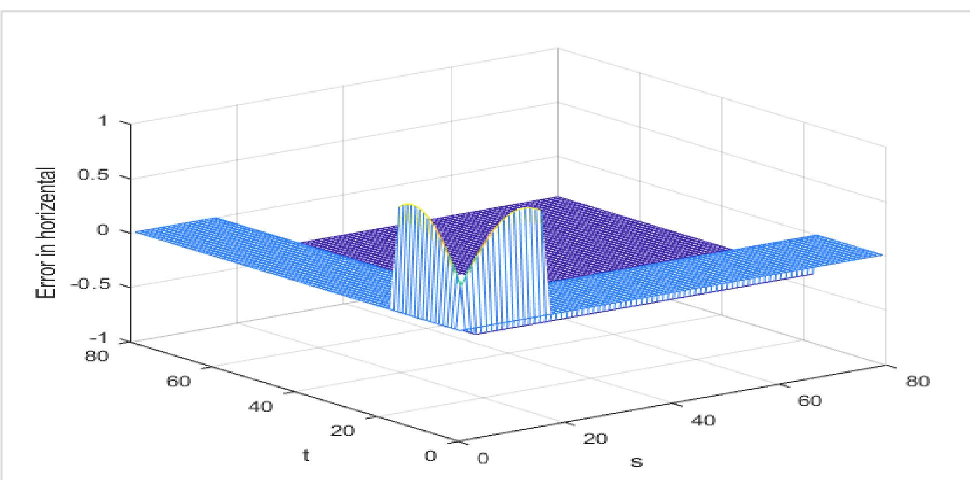


**Figure 6** Error signal in horizontal state with preview length ( $M_r = 2$ )

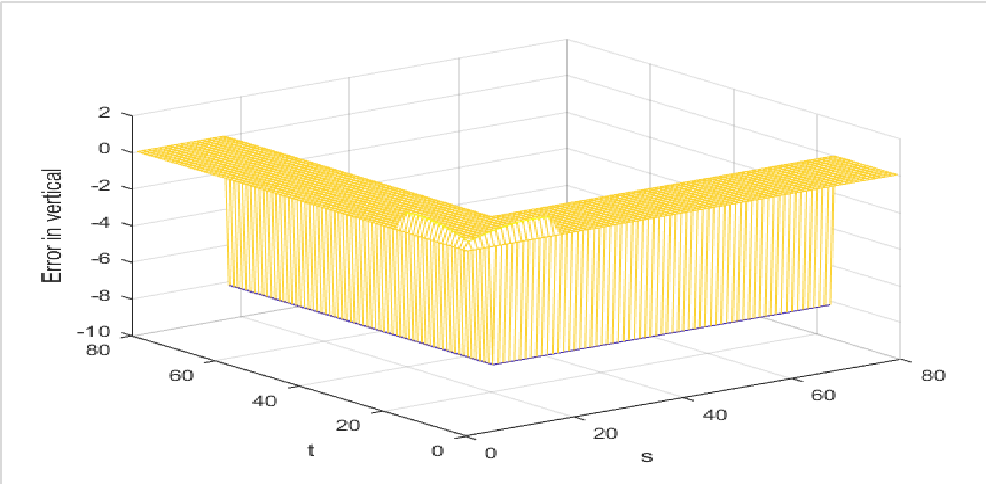


**Figure 7** Error signal in vertical state with preview length ( $M_r = 2$ )

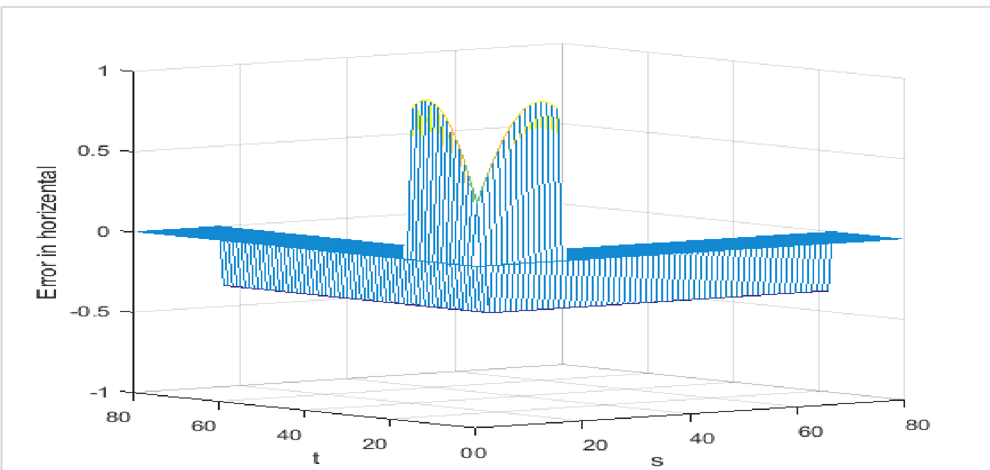


**Figure 8** Error signal in horizontal state without preview length ( $M_r = 0$ )

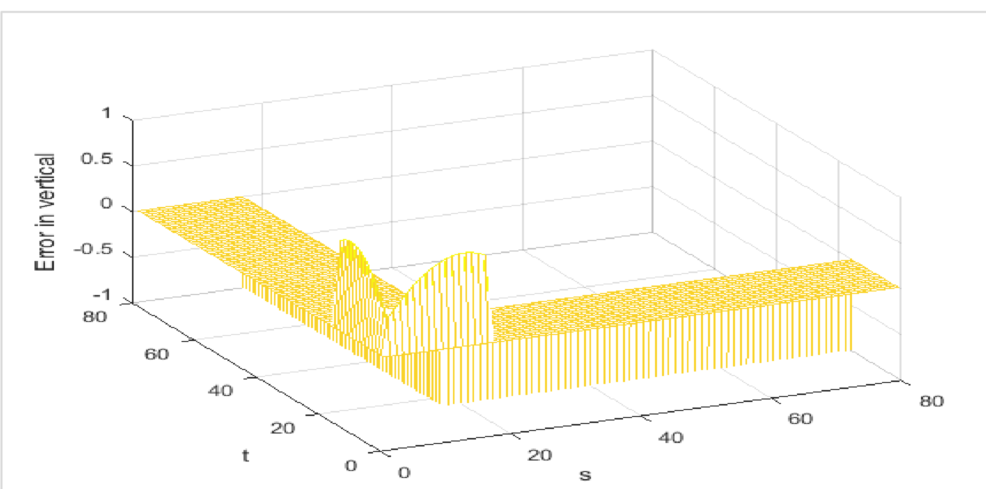


**Figure 9** Error signal in vertical state without preview length ( $M_r = 0$ )

## 5. Discussion

The 2-D DT system in Equations 1-2 considers the Roesser model with disturbance, where input variables indicate the system's external inputs and the state variables represent system's internal state.

The matrix variables $X_{1,}$ $X_{2,}$ $Y_1$ and $Y_2$ play an important role in finding controller gain. The YALMIP toolbox [23] can be used to determine whether the condition in Theorem 1 is true.

In applications with considerable time delays or norm-bounded uncertainties, preview control can be a useful technique for enhancing the performance of DT systems. However, careful evaluation of the system model, measurement quality, preview horizon length, and control settings are necessary for preview control to be feasible and stable. The preview control problem of 2-D Rosser model has been investigated without disturbances in the past. The results shown in this paper consider the preview control problem for a 2-D Roesser model with disturbances. The results validated the feasibility and stability of the above-mentioned problem. The feedback control mechanism is described by Equation 35. The 1$^{st}$ term compensates for tracking error, the 2$^{nd}$ term involves state feedback, and the difference between the 3$^{rd}$ and 4$^{th}$ terms indicates preview action based on future information about the desired tracking signal. The 5$^{th}$ term accounts for preview action considering future information about the exogenous disturbance, while the 6$^{th}$ term addresses integral action for horizontal state tracking static error.

Subsequently, the 7$^{th}$ term deals with tracking error compensation, the 8$^{th}$ term involves state feedback, and the difference between the 9$^{th}$ and 10$^{th}$ terms indicates preview action based on future information about the desired tracking signal. The 11$^{th}$ term addresses preview action considering future information about the exogenous disturbance, the 12$^{th}$ term accounts for integral action for vertical state tracking static error, and the last term compensates for initial and final value discrepancies.

**Remark:** As per the author’s knowledge, the proposed method was not used in previous literature for stabilizing the preview control system of 2-D Roesser model with disturbances. So, it is not possible for the authors to compare the error impacts.

### 5.1Limitations

The proposed method performed smoothly for the 2-D Roesser model in the presence of disturbances. However, there may be some limitations of the proposed method in the presence of system uncertainties and delays. These possible limitations are explained as follows:

Practical systems may encounter parameter uncertainties due to variations in their parameters, potentially resulting in system instability. Additionally, the system is affected by time delays, which can lead to undesirable transient responses and further contribute to potential instability. A complete list of abbreviations is shown in *Appendix I.*

## 6. Conclusion and future work

This study effectively validated the comprehensive utilization of preview information from the reference signal and disturbance signal, demonstrating the feasibility and stability of preview tracking control for 2-D DT systems. To extend preview control theory from 1-D systems to 2-D systems, an AE system was constructed. This AE system included state variables that not only encompassed error signals and preview information but also integrated a discrete integrator aimed at eliminating static errors. The controller's objective was to facilitate preview tracking control for 2-D systems, ensuring asymptotic stability. The Lyapunov method was employed to derive the LMI condition for achieving asymptotic stability in the AE system under state feedback, providing the basis for designing a preview controller.

Preview control, as an approach, capitalizes on future reference inputs to enhance system performance. Future research in preview control for 2-D DT systems could involve developing more advanced algorithms for anticipating and integrating future inputs into the control strategy. To further improve the performance of 2-D DT systems, researchers might explore synergies between preview control and other methods like model predictive control. Additionally, research avenues include tailoring preview control for specific types of 2-D DT systems, such as those used in robotics or aerospace applications, or enhancing its robustness to uncertainty and disturbances.

### Acknowledgment

We thank the anonymous reviewers for their valuable comments and suggestions.

### Conflicts of interest

The authors have no conflicts of interest to declare.

## Author's contribution statement

**Akhilesh Kumar Ravat:** Formulation of problem, analysis of designed method, validation of results writing of draft. **Amit Dhawan:** Conceptualization of the problem, methodology and validation of results. **Manish Tiwari:** Conceptualization of the problem, methodology and validation of results. **Sumit Kumar Jha:** Conceptualization of the problem, methodology and validation of results.

## References


[1] Gohrle C, Schindler A, Wagner A, Sawodny O. Design and vehicle implementation of preview active suspension controllers. IEEE Transactions on Control Systems Technology. 2013; 22(3):1135-42.

[2] Li P, Lam J, Cheung KC. Multi-objective control for active vehicle suspension with wheelbase preview. Journal of Sound and Vibration. 2014; 333(21):5269-82.

[3] Birla N, Swarup A. Optimal preview control: a review. Optimal Control Applications and Methods. 2015; 36(2):241-68.

[4] Cao R, Lu Y, Zhen Z. Tracking control of transition window for aerospace vehicles based on robust preview control. Aerospace Science and Technology. 2021; 114:106748.

[5] Suzumura A, Fujimoto Y. Real-time motion generation and control systems for high wheel-legged robot mobility. IEEE Transactions on Industrial Electronics. 2013; 61(7):3648-59.

[6] Sheridan TB. Three models of preview control. IEEE Transactions on Human Factors in Electronics. 1966:91-102.

[7] Tomizuka M. Optimal continuous finite preview problem. IEEE Transactions on Automatic Control. 1975; 20(3):362-5.

[8] Cui L, Liao Y, Zheng D. A design method of preview controller for discrete-time systems with multiple input delays. Journal Europeen Des Systemes Automatises. 2018; 51(1-3): 75-87.

[9] Kojima A. $H^{\infty}$ controller design for preview and delayed systems. IEEE Transactions on Automatic Control. 2014; 60(2):404-19.

[10] Middleton RH, Chen J, Freudenberg JS. Tracking sensitivity and achievable H∞ performance in preview control. Automatica. 2004; 40(8):1297-306.

[11] Marro G, Zattoni E. H2-optimal rejection with preview in the continuous-time domain. Automatica. 2005; 41(5):815-21.

[12] Mianzo L, Peng H. Output Feedback $H^{\infty}$ preview control of an electromechanical valve actuator. IEEE Transactions on Control Systems Technology. 2007; 15(3):428-37.

[13] Gershon E, Shaked U. H∞ preview tracking control of retarded state-multiplicative stochastic systems. International Journal of Robust and Nonlinear Control. 2014; 24(15):2119-35.

[14] Boyd S, El GL, Feron E, Balakrishnan V. Linear matrix inequalities in system and control theory. Society for Industrial and Applied Mathematics; 1994:1-36.

[15] Takaba K. Robust servomechanism with preview action for polytopic uncertain systems. International Journal of Robust and Nonlinear Control: IFAC-Affiliated Journal. 2000; 10(2):101-11.

[16] Fujisaki Y, Narazaki T. Optimal preview control based on quadratic performance index. In proceedings of the 36th IEEE conference on decision and control 1997 (pp. 3830-5). IEEE.

[17] Oya H, Hagino K, Matsuoka M. Observer-based robust tracking control with preview action for uncertain discrete-time systems. IEICE Transactions on Fundamentals of Electronics, Communications and Computer Sciences. 2007; 90(2):517-22.

[18] Katayama T, Ohki T, Inoue T, Kato T. Design of an optimal controller for a discrete-time system subject to previewable demand. International Journal of Control. 1985; 41(3):677-99.

[19] Yang Y, Guo C, Shen Z, Du J. A kind of robust controller for uncertain linear system LQ tracking problem. In proceedings of the 10th world congress on intelligent control and automation 2012 (pp. 2436-40). IEEE.

[20] Dhawan A, Kar H. An LMI approach to robust optimal guaranteed cost control of 2-D discrete systems described by the Roesser model. Signal Processing. 2010; 90(9):2648-54.

[21] Bachelier O, Yeganefar N, Mehdi D, Paszke W. On stabilization of 2D Roesser models. IEEE Transactions on Automatic Control. 2016; 62(5):2505-11.

[22] Tiwari M, Dhawan A. A survey on stability of 2-D discrete systems described by Fornasini-Marchesini first model. In international conference on power, control and embedded systems 2010 (pp. 1-4). IEEE.

[23] Ravat AK, Dhawan A, Tiwari M. LMI and YALMIP: modeling and optimization toolbox in MATLAB. In advances in VLSI, communication, and signal processing: select proceedings of VCAS 2019 (pp. 507-15). Springer Singapore.

[24] Roesser R. A discrete state-space model for linear image processing. IEEE Transactions on Automatic Control. 1975; 20(1):1-10.

[25] Bhatia AK, Ju J, Ziyang Z, Ahmed N, Rohra A, Waqar M. Robust adaptive preview control design for autonomous carrier landing of F/A-18 aircraft. Aircraft Engineering and Aerospace Technology. 2021; 93(4):642-50.

[26] Ruscelli F, Laurenzi A, Mingo HE, Tsagarakis NG. Omnidirectional walking pattern generator combining virtual constraints and preview control for humanoid robots. Frontiers in Robotics and AI. 2021; 8:1-15.

[27] Shaked U, De SCE. Continuous-time tracking problems in an H/sub/spl infin//setting: a game theory approach. IEEE Transactions on Automatic Control. 1995; 40(5):841-52.

[28] Lu Y, Zhang X, Wang Z, Qiao L. Optimal containment preview control for continuous-time multi-agent systems using internal model principle.

International Journal of Systems Science. 2023; 54(4):802-21.
[29] Xie H, Liao F, Ge SS. Robust preview control of interconnected continuous-time systems with parametric uncertainties. Applied Mathematical Modelling. 2023; 118:107-27.
[30] Ravat AK, Dhawan A, Tiwari M. Preview control for discrete time systems. In recent trends in electronics and communication: select proceedings of VCAS 2020 (pp. 1157-66). Springer Singapore.
[31] Negm MM, Mantawy AH, Shwehdi MH. A global ANN algorithm for induction motor based on optimal preview control theory. In bologna power tech conference proceedings, 2003. IEEE.
[32] Ren J, Jiang C. Robust sliding mode preview control for uncertain discrete-time systems with time-varying delay. Proceedings of the Institution of Mechanical Engineers, Part I: Journal of Systems and Control Engineering. 2022; 236(4):772-82.
[33] Lin B, Ren J. Robust preview control of nonlinear uncertain discrete-time time-delayed singular systems via sliding mode approach. Transactions of the Institute of Measurement and Control. 2023; 45(3):440-51.
[34] Sun Q, Ren J, Fu J. Robust preview control of uncertain discrete-time TS fuzzy Markovian jump systems subject to time-varying delays via sliding mode approach. Information Sciences. 2023; 639:118980.
[35] Zhang J, Lin Y, Shi P. Output tracking control of networked control systems via delay compensation controllers. Automatica. 2015; 57:85-92.
[36] Ha QP, That ND, Nam PT, Trinh H. Partial state estimation for linear systems with output and input time delays. ISA Transactions. 2014; 53(2):327-34.
[37] Kristalny M, Mirkin L. Input/output stabilization in the general two-sided model matching setup. SIAM Journal on Control and Optimization. 2012; 50(3):1413-38.
[38] Wong PK, Xie Z, Wong HC, Huang X. Design of a fuzzy preview active suspension system for automobiles. In proceedings of international conference on system science and engineering 2011 (pp. 525-9). IEEE.
[39] Wang D, Aida K. Research on fuzzy I-PD preview control for nonlinear system. JSME International Journal Series C Mechanical Systems, Machine Elements and Manufacturing. 2003; 46(3):1042-50.
[40] Xu S, Peng H. Design, analysis, and experiments of preview path tracking control for autonomous vehicles. IEEE Transactions on Intelligent Transportation Systems. 2019; 21(1):48-58.
[41] Takaba K. A tutorial on preview control systems. In SICE 2003 annual conference 2003 (pp. 1388-93). IEEE.
[42] Ming Y, Chen D, Songyan W, Tao C. Linear extended state observer based on finite-time output feedback. Journal of Automation, 2015, 41 (1): 59-66.
[43] Xie H, Liao F, Ye F, Sun M. Decentralized robust preview control for uncertain continuous-time interconnected systems. Journal of Vibration and Control. 2023; 29(7-8):1700-12.
[44] Sun Q, Ren J. Sliding mode preview tracking control of OSL nonlinear discrete-time systems. Circuits, Systems, and Signal Processing. 2022; 41(8):4347-69.
[45] Niu X, Lu B, Feng B, Li Q. Linear parameter-varying gain-scheduled preview-based robust attitude control design for a staring-mode satellite. Aerospace Science and Technology. 2022; 129:107816.

**Akhilesh Kumar Ravat** was born in 1991 at Jaunpur, Uttar Pradesh, India. He received his Bachelor's degree in Electronics and Communication Engineering from Uttar Pradesh Technical University in 2014 and Master's degree in Digital Systems at Department of Electronics and Communication Engineering from MNNIT Allahabad Prayagraj, India in 2017. He is currently a research scholar at Department of Electronics and Communication Engineering, MNNIT Allahabad, Prayagraj, Uttar Pradesh, India.
Email: akravat1991@gmail.com

**Dr. Amit Dhawan** received his Bachelor's degree in Electronics and Communication Engineering from B. I. T., Mesra, Ranchi, India in 1988 and Master's degree in Control and Instrumentation from M. N. R. E. C. Allahabad, India in 1995. He received his Ph. D. in Electronics and Communication Engineering from MNNIT Allahabad, India. He is currently a Professor at Department of Electronics and Communication Engineering, MNNIT Allahabad, Prayagraj, Uttar Pradesh, India.
Email: dhawan@mnnit.ac.in

**Dr. Manish Tiwari** received his Ph. D. degree in Electronics and Communication Engineering from MNNIT Allahabad, Prayagraj, India. He is currently an Associate Professor at Department of Electronics and Communication Engineering, MNNIT Allahabad, Prayagraj, Uttar Pradesh, India.
Email: mtiwari@mnnit.ac.in

**Dr. Sumit Kumar Jha** received his Bachelor's degree in Electronics and Communication Engineering from Maulana Abul Kalam Azad University of Technology, West Bengal, India in 2009 and Master's degree in Control System from NIT Kurukshetra, Haryana, India in 2011. He received his Ph. D. in Control and Automation from IIT Delhi, India

in 2019. He is currently an assistant Professor at Department of Electronics and Communication Engineering, MNNIT Allahabad, Prayagraj, Uttar Pradesh, India.
Email: sumit-k@mnnit.ac.in

## Appendix I

| S. No. | Abbreviation | Description |
|---|---|---|
| 1 | 1-D | One-Dimensional |
| 2 | 2-D | Two-Dimensional |
| 3 | ANN | Artificial Neural Network |
| 4 | AE | Augmented Error |
| 5 | CT | Continuous-Time |
| 6 | DT | Discrete-Time |
| 7 | FM | Fornasini-Marchesini |
| 8 | GA | Genetic Algorithm |
| 9 | IM | Induction Motor |
| 10 | LMI | Linear Matrix Inequality |
| 11 | LQ | Linear Quadratic |
| 12 | LQG | Linear Quadratic Gaussian |
| 13 | LTI | Linear Time-Invariant |
| 14 | PID | Proportional Integral Derivative |
| 15 | SDP | Semi-Definite Programming |
| 16 | YALMIP | Yet Another Linear Matrix Inequality Parser |